Small Molecules with Anti Prion Activity

Carlo Mustazza[*a], Marco Sbriccoli[b], Paola Minosi[c] and Carla Raggi[a]

[a]*National Centre for Control and Evaluation of Medicines, Italian National Institute of Health, Viale Regina Elena 299, 00161 Roma, Italy;* [b]*Department of Neurosciences, Italian National Institute of Health, Viale Regina Elena 299, 00161 Roma, Italy;* [c]*National Centre for Drug Research and Evaluation, Italian National Institute of Health, Viale Regina Elena 299, 00161 Roma, Italy*.

*Address correspondence to this author at the Centro Nazionale Controllo e Valutazione dei Farmaci, Istituto Superiore di Sanità, Viale Regina Elena, 299, 00161 Roma, Italy; Tel: +39(0)649902385; E-mail: mustazza@iss.it.

Abstract: Prion pathologies are fatal neurodegenerative diseases caused by the misfolding of the physiological prion protein (PrP^C). That leads to a β-structure rich isoform (PrP^{Sc}) which is in fact an infective agent, as it transmits its misfolding to other normally folded PrP^C molecules. Misfolded molecules then aggregate into fibrils, whose fragmentation leads to a seeding process resulting in the replication of the agent. Moreover, binding of PrP^C to other proteinaceous fibrillary aggregates is involved in Alzheimer's disease and other neurodegenerative diseases. To date there is no available cure for prion diseases and just a few clinical trials have been made. The initial approach in the search of anti-prion agents had PrP^{Sc} as a target. However, there are different prion strains, that should arise from alternative conformations of PrP^{Sc}, so often the efficacy of the ligands is strain-dependent. That has shifted research to PrP^C ligands, which either stabilize the native conformation (chaperones), or inhibit its interaction with PrP^{Sc}. The role of transition-metal mediated oxidation process in prion misfolding has also been investigated. Another approach which seems rather promising is the indirect action via other cellular targets, like membrane domains or the protein-folding activity of ribosomes (PFAR). Also, new prion-specific high throughput screening techniques have been developed. However, so far no substance has been found to be able to extend satisfactorily survival time in animal models of prion diseases. This review describes the main features of the structure-activity relationship (SAR) of the various chemical classes of anti prion agents.

Keywords: Prions, Transmissible Spongiform Encephalopathies, Scrapie, Amyloid, Hystological dyes, Structure-Activity Relationship.

Running title: Anti Prions

1. INTRODUCTION

Transmissible spongiform encephalopathies (TSEs), or prion diseases, are a group of fatal neurodegenerative disorders affecting both humans and animals. The agent that causes TSEs was termed "prion" by S.B. Prusiner and is defined as "a small proteinaceous infectious particle that is resistant to inactivation by most procedures that modify nucleic acids" [1].

In humans, TSE diseases include Kuru, Creutzfeldt-Jakob disease (CJD), Gerstmann-Sträussler-Scheinker (GSS) disease and fatal familial insomnia (FFI). The prion diseases of animals comprise scrapie, which affects sheep and goats, bovine spongiform encephalopathy (BSE) in cattle, and chronic wasting disease (CWD), which affects deer and elk. Other species are, however, susceptible to TSEs as shown by accidental (e.g. feline spongiform encephalopathy) or experimental (e.g. rodents, non-human primates) transmissions. The main feature of prion disease is the conversion of the normal cellular form of the host encoded prion protein (PrP^C) to an abnormal isoform designated PrP^{Sc}.

PrP^C is a cell membrane protein whose physiological role has not been thoroughly determined yet [2]. It is thought to have a role in cell-cell adhesion [3], transmembrane signaling [4] and in protection of peripheral nerves from demyelination [5]. It is also involved in copper cell intake and has a copper-dependent superoxide dismutase activity. The fact that copper stimulates the endocytosis of PrP^C suggests for this protein the role of copper carrier to intracellular targets [6]. Besides, the Prp^C-copper complex promotes inhibition of the N-methyl-D-aspartate receptors via *S*-nitrosylation of cysteine residues [7]. The PrP^C is anchored to the extracellular side of the cell membrane at C-terminal Ser230 linked to glycosylphosphatidylinositol. It consists of 208 residues (numeration starts from 23 as residues 1-22 are lost in the transition from the protoprotein to the mature form). The structure comprises three α-helixes (residues 144-156, 174-194 and 200-228), a two stranded antiparallel β-sheet (residues 128-131 and 161-164) and an unstructured N-terminal domain (residues 23-127). The latter includes the octapeptide repeat region (residues 51-91) with high affinity to copper ions [8,9]. It also includes a lipophilic portion (residues 112-127) which plays a fundamental role in misfolding [10].

The PrP^{Sc} is derived from PrP^C by a post-translational process that seems to involve specific interactions between the two isoforms. The molecular mechanisms of conversion of PrP^C to PrP^{Sc} are still being determined, and there are currently two models. The refolding model proposes that the conversion occurs trough the formation of a heterodimer between PrP^C and PrP^{Sc} monomer, with the latter conformer acting as a template to induce a conformational conversion of PrP^C. The nucleation model suggests that the conversion is a nucleated polymerization reaction that is reversible and that PrP^C is converted to PrP^{Sc} only in the presence of PrP^{Sc} aggregates or oligomers. Such oligomers act as a seed to bind PrP^C and catalyze its conversion into the misfolded form by incorporation into the growing polymer. The subsequent fragmentation of PrP^{Sc} polymers increases the number of effective nuclei that can direct further conversion of PrP^C [11,12].

To date there is no available cure for prion diseases and so far just a few clinical attempts have been made to treat these diseases, or at least to provide diagnostic neuroimaging agents. A wide variety of compounds have been evaluated in *in vitro* and *in vivo* tests, but none of them has been found to be able to extend satisfactorily survival time in animal models of prion diseases [13]. These substances include anionic polymers, like pentosan polysulfate (which has been used in clinical trials by intraventricular administration, [14, 15]), sulfated glycosaminoglycans [16] and their derivatives bearing lipophilic substituents [17], and polyacrylamide substituted with sulfated

acetylglycosamine units [16]. Another class of macromolecules endowed with antiprion activity is constituted by dendrimers [18 and references therein]. Anyway, macromolecules present the major drawback of absence of blood-brain barrier permeability, so most of the research on antiprion compounds concerns small molecules.

2. HISTOLOGICAL DYES AND FLUORESCENT LIGANDS

2.1 Azo dyes

Congo red (CR) is an histochemical dye characterized by a high and selective affinity to β-structure rich microfibrils [19]. It was found to inhibit amyloid aggregation in cell cultures [20]. Intracerebral inoculation of CR in scrapie-infected hamsters [21] led to prolongation of the incubation period of the disease.

Anyway, CR is unable to cross blood-brain barrier. It also presents other drawbacks: it is not selective enough and is metabolized to benzidine (carcinogenic). Moreover, it has been found that, at 1μM concentration, it promotes PrP^{Sc} aggregation, so reversing its anti-prion activity which is displayed at higher concentrations (above 5 μM) [22]. That is related to the fact that CR binds to both PrP^{Sc} and PrP^{C} [23]. A likely interpretation is that at lower concentration it occupies only some binding sites in PrP^{C}, causing conformational modifications which increase its affinity to PrP^{Sc}. At higher concentration, instead, by binding to both PrP^{C} and PrP^{Sc}, it prevents the interaction between the two proteins.

Many structural analogues of CR have been tested on $PrP^{Sc.}$ (Figure 1).

Figure 1

In a first structure-activity relationship (SAR) study on this template [24], some azo dyes were tested on scrapie-infected mouse neuroblastoma (ScNB) cells. Both terminal aromatic systems are essential for inhibitory activity on PrP^{C} misfolding. So, molecules like **1** or Orange G were not active. Another structural requisite is the planarity of the central aromatic system. The 2,2'-dimethyl analogue of CR (**2a**) was indeed less active than the parent compound, because of the hindered rotation in diphenyl bond preventing a planar conformation of the group. Instead, in the 3,3'-dimethyl analogue (**2b**), where this effect is not present, the activity was almost unaffected by the substitution. Derivatives with a modified central linker were also tested. It was shown that the distance between the two sulfonate groups is not a critical parameter for activity. So, both **3a**, where this distance is diminished, and **3b**, where it is increased, showed activities similar to CR.

In a subsequent work [22], a series of azo dyes was tested on scrapie-infected modified mouse brain (SMB) cells. The above mentioned effect of enhanced misfolding at lower concentrations (1 μM), which was reversed at higher concentrations (100 μM), was observed for the 3,3'-disubstituted compounds **2b-d**, as well as for the analogues where the amino groups are either trifluoroacetylated (**2e**) or replaced by an hydroxyl (**2f,g**). The effect of enhancing PrP^{Sc} concentration in SMB cells was also observed for compound **2h** described in another work [25]. The same feature was showed by compounds like **4a-c** with a different substitution pattern on the naphthalene rings. Substitution of the benzidine central linker with a *para*- (**3c**) or *meta*-disubstituted (**3d**) diphenyl sulfone, gave compounds with a profile similar to that of CR, with a sensibly reduced inhibiting activity at 100 μM in the case of **3d** [22].

The research was extended to compounds bearing a carboxyl instead of the sulfonic group, in order to obtain brain-penetrable compounds. Chrysamine G presented an activity comparable to CR, whereas its analogues **5a-c** had a less favorable profile. Moreover, dose-response curve of chrysamine G did not show reversal of activity at low concentrations. This latter feature was also presented by the azo dye Sirius red.

The azo dye Chicago Sky Blue 6B stabilizes Prp^{C} conformation, leading to inhibition of its binding with PrP^{Sc} or β-amyloid [26]. However the heavy interference of this compound with cell metabolism makes it unsuitable as a drug. It could anyway find application as a specific stain agent and be a template for new ligands.

2.2 Congo Red-related molecules lacking of azo group

Other compounds have been developed based on the CR template, but lacking of azo and sulfonic groups (Figure 2), in order to improve metabolic stability and brain accessibility.

Figure 2

This is the case of BSB ((*E*,*E*)-1-bromo-2,5-bis(3-carboxy-4-hydroxystiryl)benzene), which has been tested *in vivo* in TSE-infected mice [27]. This compound was shown to bind to prion plaques and to prolong the incubation period, with variable efficacy according to the strain.

In another study [28], the azo group was replaced with a variety of bioisosteric moieties (sulfonamide, amide, imine, alkene).The resulting compounds were tested on SMB cells. An additional cell-free test was performed to establish their inhibiting activity on PrP^{Sc}-promoted PrP^{C} polymerization. Compound X-34, an histological stain agent for amyloid deposits in Alzheimer's disease [29], resulted to be ineffective. Its decarboxylated analogue **6** resulted to be very effective in inhibiting PrP^{C} misfolding, but not in the polymerization test, so it must act with a different mechanism. It has been proposed for it an antioxidant activity. A similar behavior, though with a neatly weaker activity, has been showed for compounds **7d**, **8a**, **9b**, **11b** and **11c**.The amide **7a** resulted to be active in the cell assay at 10μM. Its sulfonamide analogue **7b** showed instead a moderate activity only at 50 μM, but resulted to be effective in the polymerization inhibition test. So, for

this compound the scarce activity is likely due to the difficulty to reach the molecular target. Compounds **7c** and **7d** resulted to be active, with EC_{50} respectively of 250 and 5000 nM, so far less active than **7a** (in the range 25-50 nM). Compound **7e**, isomer of **7a**, is not active, and so are the analogues like **7f-h** with the carboxymethyl group absent, or hydrolyzed to carboxyl, or replaced with other substituents. Some compounds with a terephthalamide linker (**8a,b**) were found active but much less potent than **7a**. This was also the case of the imines **9a,b** and **10a** and of the aminomethyl derivatives **11a-c**.

A related work [30] describes the highly fluorinated imino compound **10b**. It was tested on an histological sample of GSS disease, showing a high and specific affinity with prion plaques. A lesser affinity was displayed by its aminomethyl analogue**11d** and the corresponding carboxylic acid **11e**. The complete lack of affinity of the basic ester **11f** indicates that positive charges are detrimental for binding.

2.3 Other

In Figure 3 are showed other highly conjugated substances which have been tested for antiprion activity.

Figure 3

On the base of the amyloidophilic histological stain Thioflavin T, compound BTA-1 was developed. It is a lipophilic derivative which has been used, in a radiolabeled form, as an imaging agent in a mouse model of Alzheimer's disease [31]. In TSE-infected mouse neuroblastoma cells, it was found to bind selectively to prion plaques and to inhibit PrP^{Sc} formation [27]. It was in turn the lead compound for a series of 2-styryl-benzothiazoles, benzimidazoles and benzoxazoles [32]. Among the latter, the most interesting compound was BF-168, endowed with high activity in ScN2A cell tests (IC_{50}=0.4 nM); *in vivo* tests in TSE-infected mice gave a modest extension of incubation period; in histological samples, it was observed a selective binding on prion plaques, but not on synaptic deposits.

An inhibitory effect on PrP^{Sc} replications in cells was also observed for methylene blue [33] and acridine orange [34]. The fluorescent probe for amyloid plaques FDDNP shows also a high and selective affinity for prionic plaques [35].

Another compound endowed with antiprion activity is the antiprotozoal suramin. Its action is related to a PrP^{C}-depleting effect, with a mechanism involving the formation of non-infective PrP^{C} aggregates. The latter are transferred to acidic cell compartments and easily degraded by proteases. Suramin was found to be able to delay the onset of the disease in mice [36]. Testing of suramin and its analogues like **12** on ScN2A cells allowed a more detailed insight of the inhibition of *de novo* chemogenesis PrP^{Sc} due to these substance[37]. The cell localization of this effect was identified in a post trans-Golgi network site. Comparison with analogue compounds established that the presence of the two symmetric portion is essential for activity, and so is the presence of sulfonic groups.

A series of anionic conjugated polythiophenes like **13** has been tested *in vivo* in prion-infected mice by intraperitoneal administration, leading to increase of survival time[38]. NMR and docking studies evidenced that they interact with fibrillary aggregates. This interaction involves the electrostatic attraction between lysine residues of PrP^{Sc} and the carboxylate groups of the ligand. The presence of at least five thiophene rings is also required. Compound **13** binds to PrP^{Sc} with high affinity and specificity, and it acts by stabilizing the fibrillary protein aggregates, so diminishing their frangibility which is at the base of PrP^{Sc} propagation.

3. PORPHYRINS AND PHTHALOCYANINES

Porphyrins and phthalocyanines (Figure 4) were chosen as compounds to test on PrP^{Sc} because many representatives of this class have high affinity on proteins. The interaction is often accompanied by conformational changes of the protein. Also, they have a low cytotoxicity, unlike azo dyes. The main drawbacks of these molecules consist in their high affinity to albumin and their tendency to self-aggregation.

Figure 4

In a first study, some porphyrins and phthalocyanines, both in form of metal complexes and metal-free molecules, were tested on ScNB cells [39]. A cell-free investigation on their inhibitory effect on protein misfolding was also performed. Phthalocyanine tetrasulfonate (PcTS, a mixture of isomers, all with four sulfonic groups, each on a different benzene ring but in variable positions), in both metal-free and Fe^{3+} -complex forms, reduced the cell level of PrP^{Sc} with an $IC_{50} < 1$ μM. Complexes with M = Mn^{3+}, Co^{3+}, Cu^{2+}, VO^{2+} or Ni^{2+} are less active, and those with Co^{2+}, Zn^{2+} and Al^{3+} are still less active. Metal-free deuteroporphyrins **14a-c** and their Fe^{3+} -complexes **15a,b** were also tested. Methyl esterification of **14a** to **14b** resulted to be unfavorable; Fe(III) complexation in **15a** improved activity; substitution of the sulfonic group with a glycol led to a decreased activity for the metal-free molecule (**14c**), whereas results were favorable in the case of the Fe(III) complex **15b**, which showed a good inhibitory activity (IC_{50}=1.0 μM). Therefore, for these compounds, negative charges on the periphery of the tetrapyrrole system are not a requisite for activity. Instead, a good activity can be obtained also in the case of neutral polar, or even positively charged substituents, as in compounds described below.

In the case of metal-free tetraarylporphyrins **16**, substitution of *p*-sulfonate groups of **16a** with carboxyls in **16b** had an unfavorable effect, whereas their replacement with cationic trimethylammonium moieties (**16c**) increased significantly the efficacy. The tetra-(4-pyridyl)derivative **16d** was slightly more active than **16a**, and also more active than the quaternary

derivatives **16e,f**. The quaternary derivative **16g** was on the contrary neatly more active than **16a**. Formation of iron (III) complexes enhanced considerably the activity of **16a**, **16b** and **16e** (in complexes **17a**, **17c** and **17e**), whereas had a scarce effect or the more active **16c** (in **17d**). Formation of a metal complex had a favorable effect also in the case of the Cu(II), Ni(II) and Zn(II) complexes of **16e** (**17 f-h**), whereas resulted unfavorable in the case of **17b**, the Mn(III) complex of **16a**.

Compounds PcTs, **15b** and **17e** were administered intraperitoneally to scrapie infected transgenic mice [40]. They led to increase of survival time from 50 to 300%, with efficacy decreasing in the order PcTS>**17e**>**15b**. These compounds are not brain penetrable, so their effect is due to peripheral action. This is in accord with the fact, observed in a subsequent work that intraperitoneal administration of **17e** in mice leads to increase of survival time if done before, or up to 5 week after scrapie infection, whereas it was ineffective 50 days after infection, when brain has been damaged [41]. In the latter work many porphyrins were tested in scrapie-infected mice by intracerebral injection. Compounds **16c**, **17d** and the analogous Cr(II), In(III) and Cd(II) complexes resulted to be toxic in these conditions. A significant increase of survival time was observed with **17a**, but not with its Cu(II), Zn(II) and In(III) analogues. The anilinium derivative **17d** and its Cu(II), Ni(II), Zn(II) and Pd(II) analogues were also inactive.

In a further work the effect of both metal and peripheral substituents was investigated [42]. The analogues of PcTS bearing just one or two sulfonate groups showed in both *in vitro* and *in vivo* tests an activity comparable to PcTS, confirming the negligible effects of these substituents. The effects of the metal in PcTS complexes is instead remarkable. It was found a good correlation between both *in vitro* and *in vivo* activities and the tendency of the complex to self-aggregate, with the highest activities for metal-free PcTS and Fe^{3+} and Ni^{2+} complexes, and the lowest for Al^{3+} and Mn^{3+} complexes. That seems to indicate self-aggregation as a model of the interaction of phthalocyanines with aromatic side residues of the PrP^{C}. The complex Cu^{2+}-PcTS showed a peculiar behavior, being effective in *in vitro* tests and in extending survival in mice if administered before scrapie infection, but ineffective in infected mice.

Further tests of **17e** showed that its efficacy on infected N2a cells was independent from the PrP^{Sc} strain. These results indicate the unfolded form PrP^{C} as the target of the ligand [43]. Compound **17e** was also able to prevent interaction of PrP^{C} with β-amyloid.

4. OTHER METAL ION CHELATORS AND CHELATES

Structures of these compounds are represented in Figure 5.

Figure 5

As we said in the Introduction, PrP^{C} has a role in copper metabolism and this is related to its superoxide dismutase activity. It is still unclear whether copper enhances or counteracts infectivity of PrP^{Sc} [6]. Treating scrapie-infected mice with the selective copper chelator D-penicillamine [44], led to reduction of copper level in both blood and brain. However, it was not found a significant correlation between copper levels and incubation period. More consistent data have been obtained with clioquinol [45]. This is a Cu/Zn chelator and was able to extend survival of in prion-infected mice by 60%, by slowing PrP^{C} misfolding.

Copper coordinates to PrP^{C} with different modalities depending on pH [46]. PrP^{C} is able to bind up to six Cu^{2+} ions, four in the octapeptide repeat region and two in the polar region constituted by residues 92-111. Anyway, in normal conditions PrP^{C} coordinates no more than a Cu^{2+} ion, which is bound in the latter region. At pH 5.5, mimicking endosomial compartments, Cu^{2+} is coordinated to imidazole nitrogens of His96 and His111, and also with two deprotonated amide nitrogens and sulphur of Met109 [47]. In the binding mode at pH 7, coordination with His96 is not present. Giachin *et al.* [46] showed that depletion of the Cu^{2+}-His96 interaction (by mutation or introduction of cuprizone) favors prion misfolding in infected cells. That would indicate a favorable role for Cu^{2+}, which anyway is concentration-dependent, as a Cu^{2+} excess induces PrP^{C} misfolding [48].

Misfolding of PrP^{C} to PrP^{Sc} causes a decreased affinity to copper and an enhanced affinity to manganese and zinc [49, 50]. That is accompanied with a consistent decrease of superoxide dismutase activity. It can be the reason of the oxidative neural damage which is found in prion diseases [51]. The manganese complex EUK-189, endowed with superoxide dismutase and catalase activity, has been tested *in vivo* in GSS prion infected mice [52]. It led to a significant extension of survival time and to a reduction of brain vacuolar lesions.

Neurotoxicity of PrP^{Sc} is linked with disruption of transition metal homeostasis [53]. In normal conditions, transition metal ions are present in biological systems as complexes with high affinity biomolecules. If they are present in more reactive forms, they can lead to oxidative stress. That consists in increase of the concentration of reactive species generated via electron transfer reactions [50]. Among them, the most harmful is the hydroxyl radical, which causes oxidative damage to cell membrane lipids and other biomolecules [54].

Prion protein binding to Mn^{2+} has a protective effect towards manganese-induced oxidative stress [55]. Mn^{2+} ions enhance infectivity of PrP^{Sc} [56] and induce misfolding in native Prp^{C} [57]. Treating M1000 prion-infected mice with the manganese chelator CDTA [58] led a prolongation of survival, accompanied with a reduction of brain manganese level, without effect on concentration of other metal ions.

It must be also mentioned another metal complex, the inorganic heteropolyanion salt

$(NH_4)_{17}Na[NaSb_9W_{21}O_{86}]$, known as HPA-23. It has been tested in scrapie-infected mice by intravenous injection [59]. It led to a decrease of infection and increase of survival time if administered no more than 2 hours after infection. Similar heteropolyanions (like silicotungstate or the potassium analogue of HPA-23) were found to be ineffective.

5. AMINOTHIAZOLES AND RELATED COMPOUNDS

One of the most intensively studied classes of antiprion compounds is represented by aminothiazoles and their analogues (Figure 6).

Figure 6

The starting point was the aminothiazole derivative **18a**, which has been identified as a human-PrP^C ligand from a high-throughput screening study. It has been in turn the hit for a library of 5-acylamino-oxazoles and thiazoles. The latter were screened for PrP^{Sc} formation inhibition in infected SMB cells. Compounds **18b-f** resulted to be the most active with EC_{50} ranging from 1.5 μM (for **18b,c**) to 13 μM (for **18f**) [60].

Another screening study of antiprion activity on ScN2a cells led to the 2-aminothiazoles **19** [61]. Compound **19a** and **19b** showed a fair activity (EC_{50}=2.5 and 3.9 μM respectively). At least an H-bond forming group is required on the aryl bound to the position 4 of thiazole, as shown by the inactivity of the *p*-ethylphenyl analogue. Instead, for the *p*-acetamidophenyl analogue activity is almost maintained (8.5 μM), indicating that phenolic groups are not a strict requisite. Removal of methyl of **19a** in **19c** resulted in a diminished activity, and a slightly larger decrease was given by substitution of the pyridine moiety with a *p*-benzenesulfonamide. The salicylic acid derivative **19d** was inactive, probably because of its scarce cell membrane permeability.

The SAR of this system has been furtherly investigated [62]. The first aim was the removal of catechol moiety of **19a**, as this group is a potential source of labilities (metabolic instability, toxicity, scarce brain penetrability). The dimethoxy analogue **19e** resulted equipotent with **19a**. Substitution in **19e** of the *N*-hetaryl substituent R_2 with a methyl gave an inactive compound. Unlike for the catechol analogue, removal of the methyl from the pyridyl ring resulted to be favorable, and still higher activities are reached if methyl of **19e** is shifted to the 5 (**19f**, EC_{50}=0.79 μM), or 4 positions. The analogues of **19f** with different *N*-aryl groups (phenyl, 3- or 4-pyridyl, 2-pyrimidyl, pyrazinyl) were less active. The electron-releasing effect of the methyl on the pyridine ring is not relevant, as shown by the fact that the analogues of **19f** bearing a 5-methoxy or 5-trifluoromethyl substituent show activities comparable to **19f**. Ring fusion of the 4 and 5 positions of the pyridine ring in **20a-c** led to a consistent increase of activity, especially for the isoquinoline analogue **20c** (EC_{50}=0.11 μM). The request of a specific steric arrangement is confirmed by the inactivity of the isomer of **19a** bearing an α-naphthyl.

This work was extended to a SAR study of the C-4 substituent on the thiazole ring. Removal of the *m*-methoxy group from both **19f** and **20c** was tolerated. The analogues where the thiazole ring bears at C-4 an unsubstituted phenyl or an alkyl showed scarce or absent activity, and so did the trifluoromethoxyderivative **20d**. On the other hand, comparable activities were shown by various analogues bearing a hetaryl (4-pyridyl, 3-phenylisoxazol-2-yl) in this position. An *ortho* substituent, as in **19h**, resulted to be detrimental and that seems to suggest a required coplanarity of the thiazole and 5-substituent rings. In fact, a forced coplanarity via methylene ring fusion resulted to be tolerated for **21a** and favorable for **21b** (EC_{50}=5.59 and 2.44 μM respectively). Moreover, variation of the C-4 thiazole substituent influences the SAR of the C-2 substituent. So, both **19i** and **19j** showed a fair activity (0.23 and 0.25 μM respectively), higher than their methylpyridyl or isoquinolin-3-yl analogues. Introduction of an amide linker was tolerated in the case of **19k**, but not for **20e,f**. The fact that *N*-substitution in **20g,h** is not unfavorable indicates that there is no need of H-bond donor groups.

A subsequent screening on the 2-aminothiazole template, including also pharmacokinetic features and metabolic stability [63], led to compounds **22a** and **23** (EC_{50}=1.24 and 1.85 μM respectively), whose oral bioavailability and metabolic stability were confirmed by *in vivo* tests in mice.

A further SAR study based on **22a** as the lead compound [64], showed that substitution of terminal phenyl group with various heteroaromatic or heteroaliphatic rings could give compounds with activities in the nanomolar range (EC_{50}=68 nM for **22b**, 87 nM for **22c** and 51 nM for **22d**). Replacing of methyl of **22a** with other groups like in **22e** had only minor effects instead. Introduction in the 3- or 4-pyridyl ring of **22b,c** of various alkoxy or amino substituents (respectively in 4 and 3 position) gave compounds with lower or comparable affinity. An unfavorable effect is also shown for *N*-oxidation of these rings, or by introduction in these moieties of a 2-methyl. Compound **22b** presented also the advantage of an high brain penetrability, unlike its isomer **22c**.

This study was extended to 2-acylaminothiazoles **24**. A reasonable activity was observed only for small acyl groups like acetyl and cyclopropylmethyl. The latter gave also the advantage of a better metabolic stability. In these compounds the requisite of the coplanarity of substituent R_1 and phenyl is essential for activity. So, derivatives like **24b** where this coplanarity is hindered are inactive. Some compounds like **24c** (EC_{50}=70 nM) result to be fairly active but with a poorer brain penetrability with respect to diphenyl derivative **24a**.

A docking model for the binding of 2-aminothiazole derivatives with PrP^C has been recently developed [65]. The model was confirmed by its fairly good correlation with experimental data. The binding site is a cavity of

PrP^C known as pocket D [66]. In this model, interaction with compound **20b** is dominated by hydrophobic contacts, involving the quinoline, thiazole and dimethoxyphenyl systems, but hydrogen bonds involving methoxyl groups play also a role. The binding must also maintain the salt bridge between Arg156 and Glu196. This docking study led to new ligands like **25** (with a binding constant of 15.5 μM).

One of the major drawbacks of 2-aminothiazoles is due to their metabolism leading to reactive intermediates [67]. This liability is moderated by electron-withdrawing substituents. A greater concern comes from experiments with infected mice, where aminothiazole **22a** induced the formation of drug-resistant strains of PrP^{Sc} [68]. Further experiments showed that this induction is not always observed, but depends on the PrP^{Sc} strain responsible of the initial infection [69].

A series of 5-thiazolecarboxamides **26** with antiprion activity *in vitro* was developed by Thompson *et al.*[70]. This scaffold was obtained from reversal of the amido group in the series **18**. Compounds **26a-c** presented an appreciable *in vitro* activity (EC_{50}=4.0 to 4.9 μM on SMB s15 cells) which was however accompanied by cytotoxicity. Analogues with cyclic amines (pyrrolidine, morpholine) replacing the dialkylamino terminal group gave poorer results, and so did other compounds with various substituents on the amide nitrogen (labeled as R_1 in the formula), with the remarkable exception of **26d** (EC_{50}=0.43 μM). The latter showed no cytotoxicity, but presented the drawback of high metabolic instability. Many strict analogues of **26d** (like those with the furane ring methylated or substituted by thiophene or tetrahydrofuran) were inactive. The investigation was extended to 1,2,4-thiadiazoles like **27** (EC_{50}=1.62 μM). Also in this series, like in the previous compounds, a general preference for electron-releasing substituents on aromatic rings was evidenced, whereas electron-withdrawing substituents were detrimental for antiprion activity. Surface plasmon resonance (SPR) experiments showed for many of these compounds (with the exception of **26b**) a low affinity for PrP^C, so their action must be mediated by another biomolecular target. A prosecution of this study [71] led to derivatives **26e-f** and **28**, endowed with higher activity (EC_{50}=1.9 to 2.9 μM) than the hit compound **26a**, and not cytotoxic at the effective concentration.

6. ACRIDINES, QUINOLINES AND ANALOGUES

6.1 Compounds bearing a single pharmacophore unity

The prototype of these compounds (Figure 7) is the antimalarial drug quinacrine. It was found to inhibit PrP^{Sc} accumulation in ScNB cells with an EC_{50} = 0.4μM [72].

Figure 7

The effect was thought to be related to the interference with the interaction between PrP^{Sc} and glycosaminoglycanes, along with modification of lysosomal pH. A SAR study on a series of acridines, phenothiazines and quinolines [73] showed an about 10-fold lesser efficacy for the antipsychotic chlorpromazine and for the antimalarial chloroquine. No activity was found for compounds lacking of the central aliphatic chain like 9-aminoacridine. Promazine and acepromazine resulted to be slightly less effective than chlorpromazine, and a further decrease of activity was shown by promethazine, bearing a shorter side chain. The major role of the side chain in binding was confirmed in the quinacrine analogues **29**. Compounds **29a,b** lacking of a second basic nitrogen on the side chain were about 10 times less effective than quinacrine. The introduction of an ethereal oxygen (**24c**) or an aromatic or heteroaromatic ring (**24d,e**) led to inactive compounds.

An NMR study [74] identifies in the residues Tyr225, Tyr226 and Gln227 of human PrP^C the binding site of quinacrine. These residues belong to the helix α3. The efficacy is not related only to the stability of the quinacrine-PrP^C complex (whose dissociation constant is about 10^4 times larger than EC_{50}), but also to the selective accumulation of the drug in cell organelles.

An appreciable antiprion efficacy was shown also for quinine (IC_{50}= 6 μM) and other related *Cinchona* alkaloids. That prompted to the synthesis of other quinolinic compounds [75] like **30** (IC_{50}=0.45 μM). An activity in the nanomolar range was found for 4-substituted quinolines with a simpler structure, like the styrylderivative **31** (IC_{50}=12 nM).

A study on an 9-aminoacridine library [76] showed that cytotoxicity of quinacrine analogues was dependent on the substitution pattern on acridine system. Instead, antiprion effect was related to the side chain and was disfavored by the presence in the latter of phenyl rings. So, **32a** showed an EC_{50}=0.4 μM, slightly more potent than quinacrine, and with a reduced cytotoxicity. The analogue **32b** resulted clearly less potent (EC_{50}=7.1 μM).

A further study involved a library of acridines, quinolines and quinazolines bearing an arylamino substituent [77]. A preliminary screening on PrP^C affinity showed higher affinities for the 9-arylaminoacridine series than for the analogues 2-methyl-4-arylaminoquinolines and 2-phenyl-4-arylaminoquinazolines. The latter series also displayed a different SAR profile than the two former ones, suggesting a different binding mode. So, whereas the binding affinity of **33a** was suppressed by *N*-methylation (in **33b**), the same structural modification from **34a** to **34b** let affinity unaffected. No affinity or antiprion activity was found for 4-arylaminopyridine analogues, indicating that at least a benzo-fused ring was necessary. Electron-releasing substituents on aryl had a favorable effect in both acridine (as in **33c,d**) and quinoline series (*e.g.* in **34d** compared to **34c**), whereas they had no relevant effect in the quinazoline series. Screening for antiprion activity on SMB cells showed

that the NH group was necessary for activity and that electron-releasing substituents were favorable. An appreciable antiprion activity at concentrations significantly lower than the cytotoxic ones was observed only for a few compounds like **34d** (IC_{50} about 2.5 μM).

An investigation on quinolines analogues of chloroquine [78] showed for these compounds a similar SAR profile for antimalarial and antiprion activity. So, it was hypothesized for the two activities a similar mechanism at a subcellular level. It may involve cholesterol redistribution from plasma membrane to endosomal or lysosomal compartments. This study describes the series of chloroquine analogues **35** bearing a piperazine unit on the side chain. In this series, antiprion activity requires an aromatic substituent on the terminal position, as showed by the inactivity of **35a,b**. Activity was also scarce or absent in compounds like **35c,d** bearing an unsubstituted phenyl. A sensible improvement was obtained if it was replaced by a thiophene ring, as in **35e** (EC_{50}=100 nM) or **35f** (EC_{50}=90 nM). Better results are obtained if the phenyl carried electron-releasing and lipophilic substituents (**35f** and **35g** had EC_{50} respectively 75 and 50 nM) or was condensed in a naphthyl system (**35i**, EC_{50}= 75 nM). Polar substituents as in **35j,k** were instead detrimental.

A screening on a library of quinacrine analogues was performed on different prion strains [79]. Compound **36a** showed a good activity in ScN2A cell test (EC_{50}=21 nM), resulting more active and less cytotoxic than its analogues with a longer polymethylene chain. It however showed no activity in tests with other mouse cell lines transfected with human prion strains. On the other hand, derivatives **36b-d** were less active in ScN2A test (EC_{50} were respectively 0.1, 0.29 and 0.42 μM), but displayed an appreciable activity on the other strains. They were in turn the lead compounds for the prosecution of this study [80]. The SAR trend which was observed indicated the requirement of both aryl and basic heteroaliphatic systems in the side chain. In fact, no activity on mouse F3 cells infected with a human prion strain was observed for both **36e**, where the benzene ring was replaced by a bioisosteric alkyne system, and **36f**, lacking of the basic group. These latter two compounds showed however activity on ScN2A cells, as did the previously investigated **36g**.

A significant activity improvement on both strains, with respect to lead compounds, was reached for **36h** (EC_{50}=0.19 and 0.13 μM respectively on T3 and ScN2A). Its analogues with three methylene units, or with a para-methyl substituent showed a reduced activity. The analogues of **36d** with the piperidine ring replaced by nortropane, or with a para-methyl substituent, or else with a 7-chloroquinoline or 7-chloro-1,2,3,4-tetrahydroacridine replacing the acridine system showed an appreciable antiprion activity. The presence of other para-phenyl substituents (chloro, methoxy, cyano) was detrimental. With respect to the structure of **36d**, the template of **36b** resulted less tolerant to structural modifications. In fact, its analogues with an ethyl or acetyl replacing the terminal methyl were inactive on T3, whereas insertion of a methylene or carbonyl unit between benzene and piperidine rings was tolerated. The presence of the terminal basic nitrogen was instead not necessary, as the piperidine analogue **36i** (EC_{50}=0.64 and 0.10 μM respectively on T3 and ScN2A) is almost equipotent with **36b**.

The quinolizidine analogue **36j** [81] was found to be able to reduce consistently the neurotoxicity of the fragment 90-231 of the human prion protein to SH-SY5Y human neuroblastoma cells. The effect is not present for analogues lacking of the methylene bridge between the acridine and quinolizidine units, or with a longer distance between these units, or else with a different configuration at C1 of quinolizidine, but was also present, in a lesser degree, for the reactive compound **37**. This effect was found to be related to an attenuation of the resistance to protease of the prion fragment induced by **36j**.

6.2 Polyvalent ligands

The research of the analogues of the above mentioned compounds was extended to analogues bearing two or more pharmacophoric unities (Figure 8).

Figure 8

A SAR study was made on quinacrine analogues **38** bearing two acridine units [82]. If the linker was a polymethylene unit, as in **38a**, the activity was lower than in the analogues with a polyether (as **38b**) or polyamine linker (as **38c**), suggesting a favorable effect of hydrogen bonds. Comparison of linkers with different length indicated an optimal distance between the two amine nitrogens linked to the acridine systems in the range of 10-16 Å. Compound **38a** gave in preliminary tests a consistent reduction of PrP^{Sc} in ScN2a cells, but showed also a high cytotoxicity, which was much lower for **38b** (EC_{50}=25 nM) and for analogues **32d,e** (with EC_{50} values respectively 40 and 30 nM) with a less flexible linker. Azasubstitution, like in **38f**, reduced both activity and cytotoxicity.

Other bivalent PrP^{C} ligands include quinine analogues [75] like **39** (IC_{50}=3.5 μM). The presence of two quinoline units combined with the introduction of an anthraquinone system in compound **40** led to a strong increase of activity (IC_{50}=10 nM). A still stronger *in vitro* efficacy was shown for 2.2'-biquinoline **41a** (IC_{50}=3 nM). Its modification by double aza-substitution (**41b**) or introduction of two carboxyls (**41c**) resulted to be unfavorable. The high efficacy of **41a** was not related with its metal-chelating property. That was demonstrated by the fact that the addition of various metal ions to the cell culture medium was unable to modify the activity of **41a**. Moreover, other metal-chelating quinolines like 8-hydroxyquinoline resulted to be ineffective. Despite of its high efficacy *in vitro*, **41a** resulted to be less effective than quinine or quinacrine in prolonging incubation period in infected mice.

Other developed compounds include chimeric molecules derived from quinacrine and desipramine, like quinpramine (EC_{50}=85 nM) [83] and its analogue **42** (EC_{50}=20 nM) [84].

As it concerns polyvalent chloroquine analogues [78], this oligomerization led in some cases to a modest improvement of the activity as in **43** (EC_{50}=3 μM in ScN2A cells), and in other cases to inactive compounds like **44**. Appropriate linker systems can be favorable as in **45** (EC_{50}=0.5 μM).

In compound **46** (EC_{50}=0.17 μM on ScGT1 cells) [85], the linker includes a 2,5-diamino-1,4-benzoquinone moiety. It confers antioxidant properties and furnishes a planar lipophilic scaffold interacting with Phe residues of PrP^C . This interaction prevents misfolding. Comparison with analogues shows that the chlorine substituent, even if is a source of cytotoxicity, is necessary for activity. The bivalent structure and the appropriate length of the linker play also a fundamental role.

Trimeric quinacrine derivatives with a central trimesic acid unity like **47** [25] present appreciable antiprion activity *in vitro* at submicromolar concentrations. Tetrameric analogues with a porphyrin core like **48** are instead inactive, likely due to their inhability to reach endolysosomes.

7. COMPOUNDS WITH CHAPERONE ACTIVITY TARGETING THE NATIVE PRION PROTEIN

The development of a new series of antiprion compound was made on the base of genetic studies [86] which identified Gln168, Gln172, Thr215 and Gln219 as the amino acid residues of human PrP^C involved in misfolding to PrP^{Sc} and in the interaction between the two forms. There are PrP^C mutations involving at least one of these groups, including some naturally occurring in humans [87], leading to resistance to prion infection. This was the base for an *in silico* screening of PrP^C ligands leading to conformational modifications of PrP^C involving the above mentioned residues [88]. This study led to compounds Cp-60 and Cp-62 (Figure 9), which in *in vitro* tests (ScN2a cells) showed respectively an IC_{50} of 18 and 30 μM accompanied by low cytotoxicity.

Figure 9

Further investigations on antiprion compounds sharing with Cp-60 the 3,5-dicyanopyridine scaffold led to the more active compounds **49** (active at 24 μM) [89] and **50** (EC_{50}=2.5 μM) [88]. May *et al.* [90] on the base of a high-throughput screening study established a docking model for the chaperone activity of these compound on PrP^C. It involves an interaction between Thr215 and the lipophilic substituent at C4, whereas the vicinal amino and cyano groups give rise to polar interactions with Gln219, the other cyano substituent binds to Gln172 and the terminal portion of the substituent at C6 with Gln168. It was established that the interaction was favored by a halo-substituted phenyl at C-4 and by a 2-(*N*,*N*-dialkylamino)ethyl group bound to sulphur, as in the case of **51** (EC_{50}= 4.5 μM). Some bicyclic analogues i.e. thieno[2,3-*b*]pyridine-5-carbonitriles like **52** (EC_{50}= 10.9 μM) were also tested.
It was also performed a docking study of the ligand **53** with PrP^C [91]. It showed hydrogen bonds between the ligand and the residues Tyr128, Asp167, Tyr169 and Arg164 which, as it concern the first three residues, involved the cyano groups of **53**. The presence of the two aromatic or heteroaromatic rings is fundamental in docking, as shown by the inactivity of some analogues where one of these substituents was absent or replaced by an aliphatic substituent.

Kuwata *et al.* [92] performed a high-throughput *in silico* screening for PrP^C chaperones. The most significant compounds were tested on mouse neural cells infected with human TSE. The most active compound, GN8, was tested *in vivo* by subcutaneous administration in infected mice leading of increased survival time. Docking models, supported by NMR experiments, showed hydrogen bonds of this ligand with the residues Asn159 and Glu196, as well as interaction with Val189, Thr192 and Lys194. The overall effect of keeping together different helical portions of the PrP^C protein stabilized its conformation, as confirmed by circular dichroism experiments. An extensive SAR study with GN8 as lead compound [93] showed that the activity (observed *in vitro* on mouse GT1-7 cells infected with a modified human GSS agent) was enhanced by substituents on the methylene unit, like in compounds **54a,b** (both with IC_{50}=0.51 μM, about 3-fold more potent than GN8). That is related to a chaperone effect on PrP^C, as evidenced by a thermal denaturation experiment. The effect of the substituent was attributed to the restraint to the dihedral angle between the phenyl rings due to the more rigid conformation. Other structural modification of the GN8 molecule led either to derivatives with comparable activity (*e. g.* if the methylene bridge was replaced by oxygen or carbonyl, of if the amide groups were reduced to amine), or to less active or inactive compounds. Such was for example the effect of removal of one or both pyrrolidine groups, or their substitution with cyclopentyl or with bulky amine residues (i.e.dicyclohexylamine), or hetaryl groups like 1-imidazolyl, or amines bearing electronegative substituents like fluorine or hydroxyl.

The diketopiperazine **55** (EC_{50}=4.1 μM in ScGT1 cells) was developed by Bolognesi *et al.* [94] on the basis of other antiprion compounds (including Congo Red and suramin) characterized by two symmetric aromatic unities. Comparison with similar compounds bearing different aryl or heteroaryl residues evidenced that the stabilization of the planar conformation, due to intramolecular hydrogen bonds between aza groups and amide hydrogens, had a preminent role for activity. The compound resulted to be active in inhibiting PrP^C polymerization in a cell-free essay, so its action is due to conformational stabilization of PrP^C. The analogue **56**, though less active, is a potential fluorescent probe for PrP^{Sc}.

Hosokawa-Muto *et al.* [95] performed an *in silico* high-throughput screening for PrP^C chaperones, followed by testing of the most promising compounds in murine cells. One of the compounds that seemed more promising was the tetrahydrocarbazole derivative **57** (IC_{50}=8.54 μM). A subsequent SAR study on this hit compound [96] showed that the presence of a tricyclic system is essential for the activity, as shown by the inactivity of the indole and pyrrole analogues. Instead, both keto group and ring methyl are not essential. The side chain is essential for activity, and a longer chain is not favorable. Within this side chain, both amino and hydroxyl group are fundamental for activity. The hydroxyl group is likely to act mostly as a H-bond acceptor, at its *O*-methylation is tolerated. If the terminal amino group is secondary, the activity is improved, especially for *N*-benzyl derivatives. The SAR study on the benzyl group showed that electron-releasing substituents (MeO, Me) had a negligible effect on activity, whereas aza-substitution or electron-withdrawing groups (halogens, CF_3) are unfavorable, with the relevant exception of halogens in the *ortho* position. Substitution of phenyl with α-naphtyl is unfavorable, likely due to steric reasons. That led to compound **58** (EC_{50}=1.11 μM). It is active on both scrapie- and GSS-infected murine cells.

A high-throughput *in silico* screening based on the innovative docking model NUDE running on supercomputers led to compounds NPR-053 and NPR-056 [97]. Their high affinity for PrP^C was confirmed by plasmon surface resonance experiments. Docking model show for these compounds a binding modality different from GN-8, with a greater involvement of interaction with lipophilic residues. *In vitro* experiments on murine cells show reduction of PrP^{Sc} without interference on PrP^C expression. Intracerebral administration to infected mice led to a significant reduction of PrPSc brain accumulation, but without effect on survival.

A natural antioxidant showing anti-prion activity on ScN2A cells is curcumin [98]. It binds to both PrP^{Sc} and to a partially folded intermediate conformation of PrP^C [99]. A docking model was obtained for the binding interaction between curcumin and PrP^C [100]. It involves two hydrogen bonding, one between a keto group and Lys197 and another between a phenolic hydroxyl and Tyr165. The latter work shows a more effective binding mode between PrP^C and another food component, the 3,4-dimethoxycynnamic acid which is present in coffee. It interacts via hydrogen bonds between the carboxylate group and Arg139 and Asn162, along with hydrophobic interactions of the remaining part of the molecule with residues on the H3 domain. The better efficacy of this compounds, which has the additional advantage of a better bioavailability, in stabilizing PrP^C conformation has been confirmed by *in vitro* tests.

Conformational stabilization of the native prion protein has also been observed for chemical chaperones (glycerol, dimethyl sulfoxide, trimethylamine *N*-oxide) [101] and for β-cyclodextrin [102]. The effect of the latter is likely due to its binding with the lipophilic portion of Prp^C which prevents its interaction with the misfolded form.

8. INHIBITORS OF THE PROTEIN-FOLDING ACTIVITY OF RIBOSOMES (PFAR)

A major breaktrough in the research of antiprion agents was given by the development of screening methods based on yeast prions [103,104]. It provides a safer, cheaper and more rapid method for investigation of antiprion activity, compared to the previous ones based on mammalian cells. The good correlation between the results obtained with this method and with the previous ones suggests an outstanding analogy in biochemical mechanisms involving prion protein in yeast and mammals (that was lately identified with the PFAR, see below).

A previous screening with yeast prions led to the identification of a new chemical class of antiprion compounds endowed with stronger efficacy than quinacrine and chlorpromazine, which present a moderate efficacy in yeast prion test [103]. They include the new chemical class of kastellpaolitines, like **59** (Figure 10). Better results have been obtained with some phenanthridine derivatives, in particular with **60a-c**. The presence of chlorine in **60b** results favorable for activity, and a stronger effect is given by trifluoromethyl in **60c**.

Figure 10

The antihypertensive guanabenz was found to have antiprion activity in a preliminary yeast prion essay and in a following test with scrapie-infected neuroglials murine cells. Its analogues with a chlorine atom replaced by H, F or Br displayed no antiprion activity. The presence of an additional chlorine in **61** resulted instead favorable. The lack of antiprion activity of other α2-receptor agonists led to rule out any correlation between the two activities. The anticholinesterase agents tacrine and hydroxytacrine showed efficacy in prion yeast test, but not in murine cell test. That constitutes an exception of the general parallelism between the two tests insofar observed, probably due to the fact that these molecules interact with yeast cells with a different mechanism. Guanabenz was tested *in vivo* in prion infected mice, leading to a slight increase of survival time [105].

Both **60a** and guanabenz were found to not interact directly with PrP^C and to not interfere with its synthesis. The action of both compounds is due to the inhibition of the protein folding activity of ribosomes (PFAR) [106]. So, the common feature in mechanism of misfolding of both yeast prion and PrP^C has been identified: in both cases PFAR is involved in the conversion of early denatured prion protein forms into β-sheet rich ones. If PFAR is inhibited, the early denatured forms are easily degraded [107].

Mutation studies on the domain V of the 23S/25S/28S rRNA of the large ribosomal subunit (which is the active site of PFAR), along with kinetic study on the inhibition of PFAR by **60a**, permitted to identify the

nucleoside residues in domain V which bind with **60a**, and to establish that it is a competitive inhibitor [108]. In a subsequent work, Banerjee *et al.* [109], along with the development of a fluorescence method for investigation of PFAR inhibition activity, performed a computational study which established that planarity of **60a-c** derivatives is fundamental for interaction with domain V, and the electron-withdrawing effect of Cl in **60b** and CF_3 in **60c** leads to extension to electron delocalization which favors the interaction with the receptor. The inactivity of **62** is due to steric hindrance to the interaction with the domain, along with reduced electron delocalization [106].

A furtherly higher PFAR-inhibiting activity has been found for the immunostimulant imiquimod [110]. Investigation was extended to the analogues **63a-c** and **64a,b**, showing a parallelism in the results obtained in yeast prion and MovS6 cells infected with ovine 127S prion strain. The methyl derivative **63a** was slightly more active than imiquimod, whereas a reduced activity was found for the chloroderivative **63b** and for the pyrazoloquinolines **64a,b**. The azasubstituted analogue **63c** was inactive. It was also demonstrated the lack of relation between the antiprion and toll-like receptor agonist activities of imiquimod, and that it does not interfere with prion protein synthesis. Intraperitoneal administration (25 mg/kg) of imiquimod to scrapie-infected transgenic mice led to about 10% increase of survival time.

A SAR study on the 6-aminophenanthridine framework showed that introduction of substituents on the amine nitrogen of **60a** led to inactive compounds, and so did aza-substitution in different positions of either of the two fused benzene rings [111]. Electron-withdrawing substituents at 8 or 9 positions in **60c-e** enhance activity **(**IC_{50}=5-10 μM in scrapie-infected MovS6 cells**)**. Also, partial hydrogenation leading to the tetrahydroderivative **65a** or the dihydroderivative **65b** resulted to be favorable (the corresponding values of IC_{50} in scrapie-infected MovS6 cells were <5 μM for the former and 1.8 μM for the latter). Parallelism between the results with yeast and murine cells was still observed, with the exception of compound **66**, active in the latter test (IC_{50}<1.8 μM) but not in the former. So antiprion activity of **66** is probably mediated by a different mechanism.

9. *N*-(ARYL- OR HETARYL)AMIDES

A high throughput screening study was performed in 2013 [112] on both stationary phase and dividing ScN2A cells. The compounds which were screened belonged to different chemical classes. For these compounds, the activity required the presence of a group of at least three conjugated aromatic or heteroaromatic rings. Conjugation between rings could happen via ring fusion, direct bond or amide bond (Figure 11).

Figure 11

Planarity of the conjugated system was an essential requisite, so both conformational flexibility and planarity-hindering substituents had a detrimental effect. The most interesting data were given by amides bearing an aromatic or heteroaromatic substituent on both carbonyl and nitrogen side. In particular, thieno[2,3-*b*]pyridines **67** were subjected to further SAR investigation. A mono-para substituted phenyl seemed to be the optimal substituent on both amide nitrogen and position 6 of thieno[2,3-*b*]pyridine. So, EC_{50} values for **67a** and **67b** on dividing ScN2A cells were respectively 0.14 and 0.10 μM, better than analogues bearing di- or trisubstituted phenyl rings. An even better performance was showed by the fused analogue **68** (EC_{50}=0.06 μM), but not by **69** (EC_{50}>10 μM), as a further evidence of the outstanding role of both planarity and conjugation.

This study was further extended to other arylamides bearing a piperazine system in order to improve solubility [113]. Compound **70** had a good activity (EC_{50}=22 nM) accompanied by a good brain penetrability. The SAR study indicated that aza-substitution on either the terminal or the N-bound aryl had a detrimental effect, and substitution of isopropyl with methyl or ethyl was also unfavorable.

Another study was aimed at obtaining analogues of Compound B (see Par. 10.1) devoid of its toxicity due to the presence of the highly reactive hydrazine group [114]. Derivative **71a** displayed a slight activity (EC_{50}=0.64 μM) on ScN2A cells, whereas its analogue with a 4-pyridyl instead of phenyl (the amide bioisoster of Compound B) was inactive. Activity was greatly enhanced by para-phenyl substituents (EC_{50}=0.12 μM for both **71** and **47c**). In order to improve metabolic stability, a cyclopropyl substituent was introduced in the oxazole ring. Compound **71d** was endowed with a good activity (EC_{50}=80 nM) accompanied with metabolic stability and brain penetrability. Most of its analogues with different phenyl substituents resulted less active, while compound **71e** was more active (EC_{50}=60 nM) but with a poor pharmacokinetic profile.

A further development concerned similar compounds where the oxazole ring was replaced by benzothiazole or benzoxazole systems or a *p*-cyano phenyl group [115]. Structural modifications of the hits **72a** and **73a** (EC_{50}=58 and 75 nM on ScN2A-cI3 cells) indicated that the SAR of the acyl group was strongly influenced by the other side of the molecule. So, for the 3-furyl analogues, **72b** had a similar activity whereas **73b** was less active. Some analogues of **72a** lacking of the 7-methyl substituent on benzothiazole, or bearing a substituent on the central benzene ring, displayed also a lower activity. Compounds **72c** and **74** presented respectively an EC_{50}=80 and 170 nM, with the advantage over **72a** and **73a** of a good brain penetrability.

The *p*-cyanophenyl derivatives were developed on the template **75a** (EC_{50}= 1.07 μM) [115]. Aza-substitution in **75b** and its 2- and 4-pyridyl analogues did not result in a major effect on activity; introduction of an electron-releasing substituent in the position labeled as

R in the formula gave instead more active compounds like **75c** (EC_{50}=55 nM) and its analogues where R was a tertiary amine group. In the latter case however the resulting compounds had the drawback of a scarce brain penetrability. Compounds **72c**, **74** and **75c** were tested *in vivo* in scrapie-infected mice, leading to doubling survival time. The effect was however not present if the infective agent was human CJD prion. *In vitro* tests showed that these compounds did not produce drug-resistant prion strains, unlike aminothiazoles.

Other compound bearing *N*-arylamide groups, but unrelated with the previous ones, are indole-3-glyoxylamides. A screening on antiprion activity of this template led to compounds with anti-prion activities in the low nanomolar range [116]. Starting from the lead **76a** (EC_{50}=1.5 μM on SMB cells), a SAR study showed that analogues derived from aliphatic amines (included benzylamines) or secondary amines were inactive, and also substitution on the 2 position of indole or *ortho* positions in the aryl suppressed activity. Substitution at indole nitrogen or meta position of the aryl group was also unfavorable, and so was replacement of aryl with α-naphthyl or various hetaryl groups. Instead, the activity was consistently enhanced by *para* substituents on the aryl ring, and H-hydrogen bond acceptor substituents like methoxyl (**76b**, EC_{50}=11 nM) resulted the most effective. A further screening showed an analogue effect for substituents like dimethylamino or morpholino or for some heteroaromatic substituents, like 1-pyrazolyl (compound **76c**, EC_{50}=1 nM). In the continuation of this study, the preference of a heteroaromatic structure for the *para* substituent was furtherly evidenced [117]. So, the 1-imidazolyl and 1,3,4-oxadiazol-3-yl analogues of **76c** presented almost the same activity of the parent compounds, compared with the 125-fold lower activity of the pyrrolidyl analogue. Introduction in this moiety of ring substituents or insertion of a methylene bridge between amide nitrogen and the heteroaryl moiety was also unfavorable, showing the request of strict steric requisites. Also, modification of the glyoxyl moiety by reduction of either carbonyl to methylene or by insertion of two methylenes between them resulted in less active or inactive compounds. The compounds of this series do not bind to PrP^C and the mechanism of their action is still unknown.

10. VARIOUS SIMPLE AROMATIC AND HETEROCYCLIC COMPOUNDS

10.1. Hydrazones and azomethinic compounds

Bertsch *et al.* [118] developed a new cell-free high-throughput screening technique for inhibition of Prp^C-Prp^{Sc} interaction. The most active compounds were furtherly tested on ScN2A cells. The majority of active compounds was characterized by the *N'*-benzylidenebenzhydrazide substructure (Figure 12), as in the case of **77** (EC_{50}=2μM).

Figure 12

A screening on antiprion activity of hydrazones with high affinity to β-amyloid led to Compound B, endowed with high activity on ScN2A cells (ED_{50}=0.06 nM) [119]. This compounds was tested in prion-infected mice where it showed oral bioavailability and a fair efficacy in prolonging survival time. Both *in vitro* and in *vivo* efficacy were however strongly dependent on the prion strain, and the diglycosylated forms of PrP^{Sc} showed to be resistant to this compounds.

A high-throughput *in silico* screening, based mainly on aminothiazole derivatives led to hydrazone **78**, showing an IC_{50}=1.6 μM on ScN2A cells [120]. It was also able to act as a fluorescent stain on PrP^{Sc} aggregates. A docking model showed that this compound fits well in the D-pocket of Prp^C. This interaction includes, along with hydrophobic contacts (like quinoline moiety with Pro158, pyrroloquinoxaline nucleus with Tyr162, methoxyl with Lys125) also three hydrogen bonds (His187 with hydrazine nitrogen, Tyr162 with bridgehead nitrogen, Gln186 with methoxyl) and a π-cation stacking (Lys194 with the tricyclic system). The most relevant feature is the conformational stabilization of the loop Arg156-Tyr162, opposing to misfolding.

Compounds **79** and **80** come from an high-throughput *in vitro* screening study on the SMB[RC040] cell line [121]. They led to a modest increase of survival time in scrapie-infected mice by intraperitoneal administration. They not interfere with PrP^C expression; cell-free *in vitro* tests showed inhibition of PrP^{Sc} replication only in the case of **79**, suggesting a different cellular target for the action of **80**.

10.2. Others

An interesting class of antiprion compounds is represented by pyrazolones [122]. Compound **81** (Figure 13) presented a high antiprion efficacy on ScN2A and F3 cells (EC_{50}=3 nM on both strains).

Figure 13

It was developed on the basis of the neuroprotective edaravone, which has however no antiprion activity. Comparison between **81** and its structural analogues showed no correlation between antiprion and antioxidant activity (indicated by oxidation potential or hydroxyl radical scavenging activity). Also, for these compounds antiprion activity was not even related to copper chelating ability or superoxide-dismutase-like activity (which was investigated for both metal-free molecules and their copper complexes).

A high-throughtput screening on a compound library based on the N-benzylidenebenzhydrazide template led to the 3,5-diarylpyrazoles. Structure optimization gave Anle 138b, which was found to be able to inhibit the formation of prion pathological aggregates both *in vitro* and *in vivo* in scrapie-infected mice [123]. This compound presents also the advantages of oral bioavailability, brain penetrability, metabolic stability and low toxicity.

The anti-viral compound DB772 showed anti-prion activity on infected sheep microglial and rabbit renal epithelial cells [124]. A subsequent SAR study on this template [125] showed similar activity, at concentrations lower than the cytotoxic, for a host of analogues characterized by a 5-member heteroaromatic ring (furan, thiophene, pyrrole or selenophene) substituted in the 2 and 5 positions by aryls or heteroaryls and bearing one or two strongly basic amidine or 2-imidazoline substituents. Compound **82** (EC_{50}=0.26 μM on scrapie-infected sheep microglia cells) is an example. The action of these compounds does not involve inhibition of PrP^C expression, so they likely counteract PrP^C-PrP^{Sc} interaction.

The *N*-arylpiperazine scaffold was one of the most promising templates which was found in early high-throughput screening studies [61]. Li *et al.* [126] performed a further investigation on these compounds. Compound **83a** showed an EC_{50}=0.71 μM on ScN2A-c13 cells. Comparison with analogues with other *para* substituents on the *N*-phenyl ring suggested an essential role for the acetyl group, likely due to its hydrogen-bond acceptor feature. Its replacement with the almost isosteric 2-oxazolyl was found to be unfavorable, whereas the benzoxazol-2-yl **84a** and benzothiazol-3-yl **84b** analogues were found to be more potent (EC_{50}=0.3 and 0.4 μM respectively). The latter two compounds presented also the advantage of a good brain penetrability and a low cytotoxicity, but with the drawback of metabolic instability. Introduction of a methyl either in 5 position of benzoxazole ring or in 4 position of pyridine ring of **84a** led to inactive compounds, likely due to steric reasons. Introduction of a fluorine in **84c** with the attempt of improving metabolic stability, led to a compound with poorer pharmacokinetic features and also lower metabolic stability, both facts attributable to its higher hydrophilicity. Other *N*-arylpiperazines developed by Leidel *et al.* [127] were tested *in vivo* in scrapie-infected mice. They led to appreciable extension of survival time in the case of compound **85a**, whereas the other derivatives **85b** and **83a,b** were less effective. The mechanism of the action of these latter compound is still unknown, and does not involve direct interaction with PrP^C and/or PrP^{Sc}, as shown by the inefficacy of these derivatives in the cell-free essays.

Ferreira *et al.* [128] performed a high-throughput screening *in silico* and *in vitro* on a series of simple aromatic compounds. This study, which comprised also the investigation of pharmacokinetic and cell toxicity features, along with test on ScN2a cells, gave the most interesting results for chalcones like **86** and 1,2,4-oxadiazoles like **87**. A docking study on murine PrP^C was also performed, which evidenced the residues involved. A binding modality similar to that of quinacrine was showed, with prevailing hydrophobic interactions. It was also shown that the protein could bind more than a molecule of ligand, with the other molecules outside the main binding site.

A different approach for the research of antiprion compounds was attempted by Ayrolles-Torro *et al.* [129]. It was based on the previous observation that:

a) The small fragment PrP(27-30), a main marker of PrP^{Sc} infection, maintains prion infectivity;
b) The neurotoxicity of amyloid aggregates is much lesser than that of smaller, soluble oligomers, so the formation of amyloid fibrils should be regarded as a protection process [130].

So, the research of compounds which could promote the oligomerization of the PrP(27-30) fragment was performed. The first step was a high-throughput *in silico* screening of PrP^C ligands with high affinity for the region of the native protein near to the disulfide bond Cys179-Cys214. The latter bound helices 2 and 3 which are retained in the misfolding process. That led to thienopyrimidines **88** and **89** which were found to be able to decrease prion infectivity *in vitro*. Compound **88** was tested *in vivo* in mice infected with the 22L prion strain, leading to extension of survival time.

11. ANTIBIOTICS, CHOLESTEROL-DEPLETING AGENTS AND STEROIDS

These classes are grouped together because it has been showed for most of these compounds a similar mechanism for anti-prion activity which involves interaction with cell membranes. The main representatives are shown in Figure 14.

Figure 14

The anticancer antibiotic iododoxorubicin was one of the former compounds tested as antiprions [131]. It was found to inhibit PrP^{Sc} fibril aggregation by intracerebral administration in scrapie-infected hamsters. This action was accompanied by prolongation of the survival time. Similar results were obtained with two other tetracyclic antibiotics, tetracycline and doxycycline [132]. NMR investigations have shown specific interactions between tetracycline and the side residues of the unstructured lipophilic portion of PrP^C [133]. These interactions counteract aggregation of Prp^{Sc} and lower its resistance to proteases. Doxycycline has been used in phase II clinical trials, but resulted to be ineffective [134]. The derivative **90** of erythromycin A [135] is also able to bind to PrP^C leading to conformational changes which inhibit its conversion to the pathological forms. The parent erythromycin A is inactive.

The polyene antibiotic filipin was found to be able to block PrP^C endocytosis in human microglia and mouse neuroblastoma cells. It also led to inhibit PrP^{Sc} replication in infected mouse neuroblastoma cells [136]. A delay in brain accumulation of PrP^{Sc} in scrapie-infected hamsters was observed following to treatment with the polyene antibiotic amphotericin B [137]. Similar results were obtained with its water-soluble and less toxic derivative MS-8209 [138]. The latter was also found to be able to delay PrP^{Sc} replication. Polyene antibiotics have a strong affinity to

sterols, such as cholesterol which is present in the detergent-resistant microdomains of cell membranes. These are the subcellular localization of both PrP^C and PrP^{Sc}, so they are the sites of PrP^{Sc} replication [139]. Experiments on the effect of amphotericin B on infected cell lines permitted to correlate its anti-prion effect with the structural modification of detergent-resistant microdomains [140]. Similar results were obtained with the cholesterol synthesis inhibitor lovastatin [141].

The involvement of membrane lipid constituents in PrP^C misfolding was confirmed by further *in vitro* experiments with squalestatin [142]. This compound was found to be able to reduce the accumulation of misfolded prion proteins in different strains of infected cells in nanomolar concentrations.

Steroids have also been tested as antiprions. Prednisone acetate was found to be able to reduce infectivity of scrapie in mice [143]; *in vitro* tests showed a measurable anti-prion activity for other steroids like budesonide (EC_{50}=0.5 µM in scrapie-infected ScN2A cells) [144]. Comparable activities were displayed by some aminosterols like **91a,b** [135]. Some of the latter like **91b** do not affect PrP^C membrane binding, so their action is thought to involve a different biological target, probably related to PrP^C regulation or metabolism. In the case of the aminosterol U18666A, *in vitro* studies demonstrated the relation of anti-prion effect with the accumulation of cholesterol in late endosomes, related to enhanced PrP^{Sc} degradation [145].

12. MISCELLANEA

A screening of a wide library of drugs and natural products was performed on ScN2A cells infected with two different scrapie strains [144]. An activity in the range 0.1-0.5 µM was displayed by the natural alkaloids bebeerine and tetrandrine and by the antipsychotic thiothixene (Figure 15).

Figure 15

Some antioxidant polyphenols, like epicatechin 3-monogallate and epigallocatechin 3-monogallate, normally occurring in various foods, showed antiprion activity in the range 0.5-1µM. They resulted to be active also in cell-free essays.

In vitro antiprion activity was also found for cysteine protease inhibitors like E64d [72]. Another approach which has been attempted consists in autophagy-inducers, like trehalose [146], the immunosuppressant tacrolimus and the histamine antagonist astemizole [147]. Astemizole led to survival prolongation in prion-infected mice, whereas trehalose was found to be ineffective.

An anti-prion effect was also found for the anti-cancer drug tamoxifen and its metabolite 4-hydroxytamoxifen [148]. These compounds present a PrP^C-depleting effect with a mechanism similar to that of suramin (see par. 2.3), accompanied by cholesterol transfer to lysosomal membranes. In contrast with previous papers, this study shows also that autophagy is increased in PrP^{Sc}-infected cells and that autophagy-stimulating drugs were found to be ineffective in depleting prion infection.

Another compound tested on prion infection is the analgesic flupirtine, with NMDA receptor antagonist activity. It was found to be able to reduce the toxicity of the fragment PrP 106-126 in rat cortical neurons [149]. That led to its use in clinical trials [150].

The aminoglycoside **92** showed a strong inhibiting effect of misfolded prion protein formation in ScN2A cells; it resulted however almost ineffective in *in vivo* tests in mice [151]. The action of this compound was independent on the strain of the misfolded protein and was related to its interference with gene regulation (in particular, with genes involved in microtubule nucleation and those stimulated by interferon).

13. CONCLUSIONS

Research of antiprion agents remains a difficult task for medicinal chemistry, despite the wide variety of chemical tested and the development of new *in vitro* screening methodologies [103,117,152] and docking models [97,153]. That is also due to the lack of an effective screening method based on human cells [154]. Just a few compounds have entered clinical trials, namely pentosan polysulfate [14,15], quinacrine [155], doxycycline [134] and flupirtine [150], always with unsatisfactory results.

The original approach of looking for PrP^{Sc}-targeting compounds cannot any more be considered promising. In fact, there are different PrP^{Sc} strains, as the pathway of the misfolding process is not univocally definite [9]. On this regard, often the efficacy of the ligands is strain dependent. That has shifted research to compounds targeting the native form PrP^C, either by acting as chaperones, that is stabilizing its native conformation, or by blocking its binding sites to Prp^{Sc} or β-amyloid. A recent review by Barreca *et al.* [156] evidences how the binding sites of various ligands within the PrP^C molecule vary outstandingly according to the chemical structure of the ligand.

The new research trends take also in account other biomolecular targets, like PFAR, cell membrane domains or various genes, besides the PrP^C-encoding one. On this regard, it must be pointed out that for several compounds (*e. g.* the glyoxylamides described in Par. 9) the biomolecular mechanism which mediates the antiprion activity has not yet been elucidated.

LIST OF ABBREVIATIONS

BSB = (*E,E*)-1-bromo-2,5-bis(3-carboxy-4-hydroxystiryl)benzene
BSE = Bovine spongiform encephalopathy
CJD = Creutzfeldt-Jakob disease
CR = Congo red
CWD = Chronic wasting disease
EC_{50} = Half maximal effective concentration

FFI = Fatal familial insomnia
GSS = Gerstmann-Sträussler-Scheinker
NMDA = *N*-methyl-D-aspartate
NUDE = Nagasaki University Docking Engine
PcTS = Phthalocyanine tetrasulfonate
PFAR = Protein-folding activity of ribosomes
PrP^{C} = Prion protein
PrP^{Sc} = Prion protein β-structure rich isoform
SAR = Structure-activity relationships
ScNB = scrapie-infected mouse neuroblastoma cells
SMB = scrapie-infected modified mouse brain
SPR = Surface plasmon resonance
TSEs = Transmissible spongiform encephalopathies

CONFLICT OF INTEREST

The authors declare no conflict of interest, financial or otherwise.

ACKNOWLEDGEMENTS

We would like to thank Mr. Leo Zanitti for technical assistance.

REFERENCES

[1]. Prusiner, S.B. Novel proteinaceous infections particles cause scrapie. *Science*, **1982**, *216*, 136-144.

[2]. Castle, A.R.; Gill, A.C. Physiological function of the cellular prion protein. *Front. Mol. Biosci.*, **2017**, *4*, 19.

[3] Solis, G.P.; Radon, Y.; Sempou, E.; Jechow, K.; Stuermer, C.A.; Malaga-Trillo, E. Conserved roles of the prion protein domains on subcellular localization and cell-cell adhesion. *PLoS One*, **2013**, *8*, e70327.

[4] Linden, R. The biological function of the prion protein: a cell surface scaffold of signaling modules. *Front. Mol. Sci.*, **2017**, *10*, 77.

[5] Bremer, J.; Baumann, F.; Tiberi, C.; Wessig, C.; Fischer, H.; Schwarz, P.; Steele, A.D.; Toyka, K.V.; Nave, K.A.; Weis, J.; Aguzzi, A. Axonal prion protein is required for peripheral myelin maintenance. *Nat. Neurosci.*, **2010**, *13*, 310-318.

[6] Pauly, P.C.; Harris, D.A. Copper stimulates endocytosis of the prion protein. *J. Biol. Chem.* **1998**, *273*, 33107-33110.

[7] Gasperini, L.; Meneghetti, E.; Pastore, B.; Benetti, F.; Legname, G. Prion protein and copper cooperatively protect neurons by modulating NMDA receptot through S-nitrosylation. *Antioxid. Redox Signal.*, **2015**, *22*, 772-784.

[8] Pastore, A.; Zagari, A. A structural overview of the vertebrate prion proteins. *Prion*, **2007**,*1*, 185-197.

[9] Singh, J.; Udgaonkar, J. B. Molecular mechanism of the misfolding and oligomerization of prion protein: current understanding and its implications. *Biochemistry*, **2015**, *54*, 4431-4442.

[10] Jobling, M.F.; Stewart, L.R.; White, A.R.; McLean. C.; Friedhuber, A.; Maher, F.; Beyreuther, K.; Masters, C.L.; Barrow, C.J.; Collins, S.J.; Cappai, R. The hydrophobic core sequence modulates the neurotoxic and secondary structure properties of the prion peptide 106-126. *J. Neurochem.*, **1999**, *73*, 1557-1565.

[11] Prusiner, S.B. Molecular biology of prion diseases. *Science*, **1991**, *252*, 1515-1522.

[12] Caughey, B. Interaction between prion protein isoforms: the kiss of death? *Trends Biochem. Sci.*, **2001**, *26*, 235-242.

[13] Cordeiro, Y.; Ferreira, N.C. New approaches for the selection and evaluation of anti-prion organic compounds. *Mini-Rev. Med. Chem.*, **2015**, *15*, 84-92.

[14] Tsuboi, Y.; Doh-Ura, K.; Yamada, T. Continuous intraventricular infusion of pentosan polysulfate: clinical trial against prion diseases. *Neuropathology*, **2009**, *29*, 632-636.

[15] Todd, N.V.; Morrow, J.; Doh-Ura, K.; Dealler, S.; O'Hare, S.; Farling, P.; Duddy, M.; Rainov, N.G. Cerebroventricular infusion of pentosan polysulfate in human variant Creutzfeldt-Jakob disease. *J. Infect.*, **2005**, *50*, 394-396.

[16] Yamaguchi, S.; Nishida, Y.; Sasaki, K.; Kambara, M.,; Kim, C.L.; Ishiguro, N.; Nagatsuka, T.; Uzawa, H.; Horiuchi, M. Inhibition of PrP^{sc} formation by synthetic *O*-sulfated glycopyranosides and their polymers. *Biochem. Biophys. Res. Commun*, **2006**, *349*, 485-491.

[17] Ouidja, M.O.; Petit, E.; Kerros, M.E.; Ikeda, Y.; Morin, C.; Carpentier, G.; Barritault, D.; Brugère-Picoux, J.; Deslys, J.P.; Adjou, K.; Papy-Garcia, D. Structure-activity studies on heparin mimetic polyanions for anti-prion therapies. *Biochem. Biophys. Res. Commun.*, **2007**, *363*, 95-100.

[18] McCarthy, J.M;, Moreno, B.R.; Filippini, D.; Komber, H.; Maly, M.; Cernescu, M.; Brutschy, B.; Appelhans, D.; Rogers, M.S. Influence of surface groups on poly(propylene imine) dendrimers antiprion activity. *Biomacromolecules*, **2013**, *14*, 27-37.

[19] Cooper, J.H. Selective amyloid staining as a function of amyloid composition and structure. Histochemical analysis of the alkaline Congo red, standardized toluidine blue, and iodine methods. *Lab. Invest.*, **1974**, *31*, 232-238.

[20] Frid, P.; Anisimov, S.V.; Popovic, N. Congo red and protein aggregation in neurodegenerative diseases. *Brain Res.Rev.*, **2007**, *53*, 135-160.

[21] Ingrosso, L.; Ladogana, A.; Pocchiari, M. Congo Red prolongs the incubation period in scrapie-infected hamsters. *J. Virol.*, **1995**, *69*, 506-508.

[22] Rudyk, H.; Vasiljevic, S.; Hennion, R.M.; Birkett, C.R.; Hope, J.; Gilbert, I.H. Screening Congo red and

its analogues for their ability to prevent the formation of PrP-res in scrapie-infected cells. *J.Gen. Virol.*, **2000**, *81*, 1155-1164.

[23] Caughey, B.; Brown, K.; Raymond, G.J.; Katzenstein, G.E.; Thresher, W. Binding of the protease-sensitive form of PrP (prion protein) to sulfated glycosaminoglycan and Congo red. *J.Virol.*, **1994**, *68*, 2135-2141.

[24] Demaimay, R;, Harper, J.; Gordon, H.; Weaver, D.; Chesebro, B.; Caughey, B. Structural aspects of Congo red as inhibitor of protease-resistant prion protein formation. *J. Neurochem.*, **1998**, *71*, 2534-2541.

[25] Mays, C.E.; Joy, S.; Li, L.; Yu, L.; Genovesi, S.; West, F.G.; Westaway, D. Prion inhibition by multivalent PrP^{Sc} binding compounds. *Biomaterials*, **2012**, *33*, 6808-6822.

[26] Risse, E.; Nicoll, A.J.; Taylor, W.A.; Wright, D.; Badoni, M.; Yang, X.; Farrow, M.A.; Collinge, J. Identification of a compound that disrupts binding of amyloid-β to the prion protein using a novel fluorescence-based assay. *J. Biol. Chem.*, **2015**, *290*, 17020-17028.

[27] Ishikawa, K.; Doh-ura, K.; Kudo, Y.; Nishida, N.; Murakami-Kubo, I.; Ando, Y.; Sawada, T.; Iwaki, T. Amyloid imaging probes are useful for detection of prion plaques and treatment of transmissible spongiform encephalopathies. *J. Gen. Virol.*, **2004**, *85*, 1785-1790.

[28] Sellarajah, S.; Lekishvili, T.; Bowring, C.; Thompsett, A.R.; Rudyk, H.; Birkett, T.R.; Brown, D.R.; Gilbert, I. H. Synthesis of analogues of Congo red and evaluation of their anti-prion activity. *J. Med. Chem.*, **2004**, *47*, 5515-5534.

[29] Styren, S.D.; Hamilton, R.L.; Styren, G.C.; Klunk, W:E, X-34, a fluorescent derivative of Congo red: a novel histochemical stain for Alzheimer's disease pathology. *J. Histochem. Cytochem.*, **2000**, *48*, 1223-1232.

[30] Mustazza, C.; Sbriccoli, M.; Borioni, A.; Ferretti, R.; Del Giudice, M.R. New fluorinated 1,4-bis(arylaminomethyl)- and 1,4-bis (arylaminomethylene)benzenes as fluorescent probes for amyloid plaques in Alzheimer's disease and transmissible spongiform encephalopathies. *Med. Chem. Comm.*, **2012**, *3*, 357-361.

[31] Mathis, C.A.; Bacskai, B.J.; Kajdasz, S.T.; McLellan M.E.; Frosch, M.P.; Hyman, B.T.; Holt, D.P.; Wang, Y.; Huang, G.F.; Debnath, M.L.; Klunk, M.E. A lipophilic Thioflavin-T derivative for positron emission tomography (PET) imaging of amyloid in brain. *Bioorg. Med. Chem. Lett.*, **2002**, *12*, 295-298.

[32] Ishikawa, K.; Kudo, Y.; Nishida, N.; Suemoto. T.; Sawada, T.; Iwaki, T.; Doh-ura, K. Styrylbenzoxazole derivatives for imaging of prion plaques and treatment of transmissible spongiform encephalopathies. *J. Neurochem.*, **2006**, *99*, 198-205.

[33] Cavaliere, P.; Torrent, J.; Prigent, S.; Granata, V.; Pauwels, K.; Pastore, A.; Rezaei, H.; Zagari, A. Binding of methylene blue to a surface cleft inhibits the oligomerization and fibrillization of prion protein. *Biochim. Biophys. Acta* **2013**, 1832, 20-28.

[34] Hyeon, J.W.; Kim, S.Y.; Lee, S.M:; Lee, J.; An, S.S.A; Lee, M.K.; Lee, Y.S. Anti-prion screening for acridine, dextran, and tannic acid using real time-quaking induced conversion: a comparison with PrPSc-infected cell screening. *PLoS One* **2017**, 12, e0170266.

[35] Bresjanac, M.; Smid, L.M.; Vovko, T.D.; Petrič, A.; Barrio, J.A.; Popovic, M. Molecular imaging probe 2-(1-{6-[(2-fluoroethyl)(methyl)amino]-2-naphthyl}ethylidene malononitrile labels prion plaques in vitro. *Neurosci. J.* **2003**, *23*, 8029-8033.

[36] Gilch, S.; Winklhofer, K.F.; Groschup, M.H.; Nunziante, M.; Lucassen, R.; Spielhaupter, C.; Muranyi, W.; Riesner, D.; Tatzelt, J.; Schätzl, H.M. Intracellular re-routing of prion protein prevents propagation of PrP^{Sc} and delay onset of prion disease. *EMBO J.*, **2001**, *20*, 3957-3966.

[37] Nunziante, M.; Kehler, C.; Maas, E.; Kassack, M.U.; Groschup, M.; Schätzl, H.M. Charged bipolar suramin derivatives induce aggregation of the prion protein at the cell surface and inhibit PrP^{Sc} replication. *J. Cell Sci.* **2005**, *118*, 4959-4973.

[38] Herrmann, U.S.; Schütz, A.K.; Shirani, H.; Huang, D.; Saban, D.; Nuvolone, M.; Li, B.; Ballmer, B.; Åslund, A.K.; Mason, J.J.; Rushing, E.; Budka, H.; Nyström, S.; Hammarström, P.; Böckmann, A.; Caflisch, A.; Meier, B.H.; Nilsson, K.P.; Homemann, S.; Aguzzi, A. Structure-based drug-design identifies polythiophenes as antiprion compounds. *Sci. Transl. Med.* **2015**, *7*, 299ra123.

[39] Caughey, W.S.; Raymond, L.D.; Horiuchi, M.; Caughey, B. Inhibition of protease-resistant prion protein formation by porphyrins and phthalocyanines. *Proc. Natl. Acad. Sci. USA*, **1998**, *95*, 12117-12122.

[40] Priola, S:A.; Raines, A.; Caughey, W.S. Porphyrin and phthalocyanine antiscrapie compounds. *Science* **2000**, 287, 1503-1506.

[41] Kocisko, D.A.; Caughey, W.S.; Race, R.E.; Roper, G.; Caughey, B.; Morrey, J.D. A porphyrin increases survival time of mice after intracerebral prion infection. *Antimicrob. Agents Chemother.*, **2006**, *50*, 759-761.

[42] Caughey, W.S.; Priola, S.A.; Kocisko, D.A.; Raymond, L.D.; Ward, A.; Caughey, B. Cyclic tetrapyrrole sulfonation, metals, and oligomerization in antiprion activity. *Antimicrob. Agents Chemother.*, **2007**, *51*, 3387-3394.

[43] Massignan, T.; Cimini, S.; Stincardini, C.; Cerovic, M.; Vanni, I.; Elezgarai, S.R.; Moreno, J.;

Stravalaci, M.; Negro, A;, Sangiovanni, V.; Restelli, E.; Riccardi, G.; Gobbi, M.; Castilla, J.; Borsello, T.; Nonno, R.; Biasini, E. A cationic tetrapyrrole inhibits toxic activities of the cellular prion protein. *Sci. Rep*., **2016**, *6*, 23180.

[44] Sigurdsson, E.M.; Brown, D.R.; Alim, M.A.; Scholtzova, H.; Carp, R;, Meeker, H.C.; Prelli, F.; Frangione, B.; Wisniewski, T. Copper chelation delays the onset of prion disease. *J. Biol. Chem.*, **2003**, *278*, 46199-46202.

[45] Ponti, W.; Sala, M.; Pollera, C.; Braida, D.; Poli, G.; Bareggi, S. *In vivo* models for the evaluation of molecules active towards transmissible spongiform encephalopathies. *Vet. Res. Commun.*, **2004**, *28*, 307-310.

[46] Giachin, G.; Mai, P.T.; Tran, T.H.; Salzano, G.; Benetti, F.; Migliorati, V.; Arcovito, A.; Della Longa, S.; Mancini, G.; D'Angelo, P.; Legname, G. The non-octarepeat copper binding site of the prion protein is a key regulator of prion conversion. *Sci. Rep*., **2015**, *5*, 15253.

[47] Arena, G.; La Mendola, D.; Pappalardo, G.; Sóvágó, I.; Rizzarelli, E. Interaction of Cu^{2+} with prion family peptide fragments: considerations on affinity, speciation and coordination. *Coord. Chem. Rev.*, **2012**, *256*, 2202-2218.

[48] Yen, C.F.; Harischandra, D.S.; Kanthasamy, A.; Sivasankar, S. Copper-induced structural conversion templates prion-protein oligomerization and neurotoxicity. *Sci. Adv*., **2016**, *2*, e1600014.

[49] Choi, C.J.; Kanthasamy, A.; Anantharam, V.; Kanthasami, A.G. Interaction of metals with prion protein: possible role of divalent cations in the pathogenesis of prion diseases. *Neurotoxicology*, **2006**, *27*, 777-787.

[50] Brazier, M.W.; Wedd, A.G.; Collins, S.J. Antioxidant and metal chelation-based therapies in the treatment of prion disease. *Antioxidants (Basel)*, **2014**, *3*, 288-308.

[51] Brown, D.R. Neurodegeneration and oxidative stress: prion disease results from loss of antioxidant defense. *Folia Neuropathol*., **2005**, *43*, 229-243.

[52] Brazier, M.W; Doctrow, S. R.; Masters, C.L.; Collins, S.J. A manganese superoxide dismutase/catalase mimetic extends survival in a mouse model of human prion disease. *Free Radic. Biol. Med.*, **2008**. *45*, 184-192.

[53] Toni, M.; Massimino, M.L.; De Mario, A.; Angiulli, E.; Spisni, E. Metal dishomeostasis and their pathological role in prion and prion-like diseases: the basis for a nutritional approach. *Front. Neurosci*., **2017**, *11*, 3.

[54] Ozcan, A.; Ogun, M.; Biochemistry of reactive oxygen and nitrogen species, in: Basic principles and clinical significance of oxidative stress, Gowder, S.J.T. (ed.), InTech (Rijeka, Croatia) 2015.

[55] Choi, C.J.; Anantharam, V.; Saetveit, N.J.; Houk, R.S;, Kanthasamy, A.; Kanthasamy, A.G. Normal cellular prion protein protects against manganese-induced oxidative stress and apoptotic cell death. *Toxicol. Sci.*, **2007**, *98*, 495-509.

[56] Davies, P.; Brown, D.R. Manganese enhances prion protein survival in model soils and increases prion infectivity to cells. *PLoS One*, **2009**, *4*, e7518.

[57] Brown, D.R.;Hafiz, F.; Glassmith, I.L.; Wong, B.S.; Jones, I.M.; Clive, C.; Haswell, S.J. Consequences of manganese replacement of copper for prion protein function and proteinase resistance. *EMBO J*,, **2000**, *19*, 1180-1186.

[58] Brazier, M.W.; Volitakis, I.; Kvasnicka, M.; White, A.R.; Underwood, J.R.; Green, J.E.; Han, S.; Hill, A.F.; Masters, C.L.; Collins, S.J. Manganese chelation therapy extends survival in a mouse model of M1000 prion disease. *J. Neurochem.*, **2010**, *114*, 440.

[59] Kimberlin, R.H.; Walker, C.A. Suppression of scrapie infection in mice by heteropolyanion 23, dextran sulfate, and some other polyanions. *Antimicrob. Agents Chemother*., **1986**, *30*, 409-413.

[60] Heal, W.; Thompson, M.J.; Mutter, R.; Cope, H.; Louth, J.C.; Chen, B. Library synthesis and screening: 2,4-diphenylthiazoles and 2,4-diphenyloxazoles as potential novel prion disease therapeutics. *J.Med. Chem.*, **2007**, *50*, 1347-1353.

[61] Ghaemmaghami, S.; May, B.C.H.; Renslo, A.R.; Prusiner, S.B. Discovery of 2-aminothiazoles as potent antiprion compounds. *J.Virol*., **2010**, *84*, 3408-3412.

[62] Gallardo-Godoy, A.; Gever, J.; Fife, K.L.; Silber, M.; Prusiner, S.B.; Renslo, A.R. 2-Aminothiazoles as therapeutic leads for prion diseases. *J.Med. Chem.*, **2011**, *54*, 1010-1021.

[63]. Silber, B.M.; Rao, S.; Kimberly, L.F.; Gallardo-Godoy, A.; Renslo, A.R.; Dalvie, D. K.; Giles, K.; Freyman, Y.; Elepano, M.; Gever, J.R.; Li, Z.; Jacobson, M.P.; Huang, Y.; Benet, L.Z.; Prusiner, S.B. Pharmacokinetics and metabolism of 2-aminothiazoles with antiprion activity in mice. *Pharm. Res.*, **2013**, *30*, 932-950.

[64] Li, Z.; Silber, B.M.; Rao, S.; Gever, J.; Bryant, C.; Gallardo-Godoy, A.; Dolghih, E.; Widjaja, K.; Elepano, M.; Jacobson, M. P.; Prusiner, S.B.; Renslo, A.R. 2-Aminothiazoles with improved pharmacotherapeutic properties for treatment of prion disease. *ChemMedChem*., **2013**, *.8*, 847-857.

[65] Pagadala, N.S.; Perez-Pineiro, R.; Wishart, D.S.; Tuszynski, J.A. *In silico* studies and fluorescence binding assays of potential anti-prion compounds reveal an important binding site for prion inhibition

from PrP^{C} to PrP^{Sc}. *Eur.J.Med.Chem.,* **2015**, *91*, 118-131.

[66] Narayanan, S.P.; Nair, D.G.; Schaal, D.; Barbosa de Aguiar, M.; Wenzel, S.; Kremer, W.; Schwarzinger, S.; Kalbitzer, H.R. Structural transitions in full-length human prion protein detected by xenon as probe and spin labeling of the N-terminal domain. *Sci. Rep.,* **2016**, *6*, 28419.

[67] Kalgutkar, A.S.; Driscoll, J.; Zhao, S.X.; Walker, G.S.; Shepard, R.M.; Soglia, J.R.; Atherton, J.; Yu, L.; Mutlib, A. E.; Munchhof, M.J.; Reiter, L.A.; Jones, C. S.; Doty, J.L.; Trevena, K.A.; Shaffer, C.L.; Ripp, S.L. A rational chemical intervention strategy to circumvent bioactivation labilities associated with a nonpeptidyl thrombopoietin receptor agonist containing a 2-amino-4-arylthiazole motif. *Chem. Res. Toxicol.,* **2007**, *20*, 1954-1965.

[68] Berry, D.; Lu, D.; Geva, M.; Watts, J.C.; Bhardwaj, S.; Oehler, A.; Renslo, A.R.; DeArmond, S.,J.; Prusiner, S.B.; Giles, K. Drug resistance confounding prion therapeutics. *Proc. Natl. Acad, Sci. USA,* **2013**, *110*, E4160-E4169.

[69] Berry, D.; Giles, K.; Oehler, A.; Bhardway, S.; DeArmond, S.J.; Prusiner, S.B. Use of 2-aminothiazole to treat chronic wasting disease in transgenic mice. *J. Infect. Dis,* **2014**, *212*, S17-S25.

[70] Thompson, M.J.; Louth, J.C.; Greenwood, G.K.; Sorrell, F.J.; Knight, S.G.; Adams, N.B.P.; Chen, B. Improved 2,4-diarylthiazole-based antiprion agents: switching the sense of the amide.

[71] Thompson, M.J.; Louth, J.C.; Little, S.M.; Chen, B.; Coldham, I. 2,4-Diarylthiazole antiprion compounds as a novel structural class for antimalarial leads. *Bioorg. Med. Chem. Lett.*, **2011**, *21*, 3644-3647.

[72] Doh-ura, K.; Iwaki, T.; Caughey, B. Lysosomotropic agents and cysteine protease inhibitors inhibit scrapie-associated prion protein accumulation. *J. Virol.,* **2000**, *74*, 4894-4897.

[73] Korth, C.; May, B.C.; Cohen, F.E.; Prusiner, S.B. Acridine and phenothiazine derivatives as pharmacotherapeutics for prion disease. *Proc. Natl. Acad. Sci. USA,* **2001**, *98*, 9836-41.

[74] Vogtherr, M.; Grimme, S.; Elshorst, B.; Jacobs, D.J.; Fiebig, K.; Griesinger, C.; Zahn, R. Antimalarial drug quinacrine binds to C-terminal helix of cellular prion protein. *J.Med. Chem,* **2003**, *46*, 3563-3564.

[75] Murakami-Kubo, I.; Doh-ura, K.; Ishikawa, K.; Kawatake, S.; Sasaki, K.; Kira, J.; Ohta, S.; Iwaki, T. Quinoline derivatives are therapeutic candidates for transmissible spongiform encephalopathies. *J. Virol.*, **2004**, *78*, 1281-1288.

[76] Klingenstein, R.; Löber, S.; Kujala, P.; Godsave, S.; Leliveld, S.R.; Gmeiner, P.; Peters, P.J.; Korth, C. Tricyclic antidepressants, quinacrine and a novel, synthetic chimera thereof clear prions by destabilizing detergent-resistant membrane compartments. *J. Neurochem.,* **2006**, *98*, 748-759.

[77] Cope, H.; Mutter, R.; Heal, W.; Pascoe, C.; Brown, P.; Pratt, S.; Chen, B. Synthesis and SAR study of acridine, 2-methylquinoline and 2-phenylquinazoline analogues as anti-prion agents. *Eur. J.Med. Chem.,* **2006**, *41*, 1124-1143.

[78] Klingenstein, R.; Melnyk, P.; Leliveld, S.R.; Ryckebusch, A.; Korth, C. Similar structure-activity relationships of quinoline derivatives for antiprion and antimalarial effects. *J.Med. Chem.,* **2006**,. *49*, 5300-5308.

[79] Nguyen, T.H.; Lee, C.Y.; Teruya, K.; Ong, W.Y.; Doh-ura, K.; Go, M.L. Antiprion activity of functionalized 9-aminoacridines related to quinacrine. *Bioorg. Med.Chem.,* **2008**, *16*, 6737-6746.

[80] Nguyen, T.H.; Sakasegawa, Y.; Doh-ura, K.; Go, M.L. Anti-prion activities and drug-like potential of functionalized quinacrine analogs with basic phenyl residues at the 9-amino position. *Eur. J. Med. Chem.,* **2011**, *46*, 2917-2929.

[81] Villa, V.; Tonelli, M.; Thellung, S.; Corsaro, A.; Tasso, B.; Novelli, F.; Canu, C.; Pino, A.; Chiovitti, K.; Paludi, D.; Russo, C.; Sparatore, A.; Aceto, A.; Boido, V.; Sparatore, F.; Florio, T. Efficacy of novel acridine derivatives in inhibition of hPrP90-231 prion protein fragment toxicity. *Neurotox. Res.,* **2011**, *19*, 556-574.

[82] May, B.C.; Fafarman, A.T.; Hong, S.B.; Rogers, M.; Deady, L.W.; Prusiner, S.B.; Cohen, F.E. Potent inhibition of scrapie prion replication in cultured cells by bis-acridines. *Proc. Natl. Acad. Sci. USA,* **2003**, *100*, 3416-3421.

[83] Dollinger, S.; Löber, S.; Klingenstein, R.; Korth, C.; Gmeiner, P. A chimeric ligand approach leading to potent antiprion active acridine derivatives: design, synthesis, and biological investigations. *J.Med. Chem.,* **2006**, *49*, 6591-6595.

[84] May, B.C; Witkop, J.; Sherrill, J.; Anderson, M.O.; Madrid, P.B.; Zorn, J.A.; Prusiner, S.B.; Cohen, F.E.; Guy, R.K. Structure-activity relationship study of 9-aminoacridine compounds in scrapie-infected neuroblastoma cells. *Bioorg. Med. Chem.Lett.,* **2006**, *16*, 4913-4916.

[85] Bongarzone, S.; Tran, H.N.; Cavalli, A.; Roberti, M.; Carloni, P.; Legname, G.; Bolognesi, M.L. Parallel synthesis, evaluation and preliminary structure-activity relationship of 2,5-diamino-1,4-benzoquinones as novel class of bivalent antiprion compound. *J. Med. Chem.,* **2010**, *53*, 8197-8201.

[86] Zulianello, L;, Kaneko, K.; Scott, M.; Erpel, S.; Han, D.; Cohen. F.E.; Prusiner, S.B. Dominant-negative inhibition of prion formation diminished by deletion mutagenesis of the prion protein. *J. Virol.*, **2000**, *74*, 4351-4360.

[87] Shibuya, S.; Higuchi, J.; Shin, R.W.; Tateishi, J.; Kitamoto T. Protective prion protein polymorphisma against sporadic Creutzfeldt-Jakob disease. *Lancet* **1998**, *351*, 419.

[88] Perrier, V.; Wallace, A.C.; Kaneko, K.; Safar, J.; Prusiner, S.B. Mimicking dominant negative inhibition of prion replication through structure-based drug design. *Proc.Natl. Acad. Sci. USA.*, **2000**, *97*, 6073-6078.

[89] Reddy, T.R.; Mutter, R.; Heal, W.; Guo, K.; Gillet, W.J.; Pratt, S.; Chen, B. Library design, synthesis and screening: pyridine dicarbonitriles as potential prion disease therapeutics. *J. Med. Chem,*. **2006**, *49*, 607-615.

[90] May, B.C.H.; Zorn, J.A.; Witkop, J.; Sherrill, J.; Wallace, A.C.; Legname, G.; Prusiner, S.B.; Cohen, F.E. Structure-activity relationship study of prion inhibition by 2-aminopyridine-3,5-dicarbonitrile-based compounds: parallel synthesis, bioactivity and *in vitro* pharmacokinetics. *J. Med. Chem.* **2007**, *50*, 65-73.

[91] Guo, K.; Mutter, R.; Heal, W.; Reddy, T.R. Cope, H.; Pratt, S.; Thompson, M.J.; Chen, B. Synthesis and evaluation on a focused library of pyridine dicarbonitriles against prion disease. *Eur. J. Med. Chem.*, **2008**, *43*, 93-106.

[92] Kuwata, K.; Nishida, N.; Matsumoto, T.; Kamatari, Y.O.; Hosokawa-Muto, J.; Kodama, K.; Nakamura, H.K.; Kimura, K.; Kawasaki, M.; Takakura, Y.; Shirabe, S.; Takata, J.; Kataoka, Y.; Katamine, S. Hot spots in prion protein for pathogenic conversion. *Proc. Natl. Acad. Sci. USA*, **2007**, *104*, 11921-11926.

[93] Kimura, T.; Hosokawa-Muto, J.; Kamatari, Y.O.; Kuwata, K. Synthesis of GN8 derivatives and evaluation of their antiprion activity in TSE-infected cells. *Bioorg. Med. Chem. Lett.*, **2011**, *21*, 502-507.

[94] Bolognesi, M.L.; Ai Tran, H.N.; Staderini, M.; Monaco, A.; López-Cobeñas, A.; Bongarzone, S.; Biarnés, X.; López-Alvarado, P.; Cabezas, N.; Caramelli, N.; Carloni, P.; Menéndez, J.C.; Legname, G. Discovery of a class of diketopiperazines as antiprion compounds. *ChemMedChem*, **2010**, *5*, 1324-1334.

[95] Hosokawa-Muto, J.; Kamatari, Y.O.; Nakamura, H.K.; Kuwata, K. Variety of antiprion compounds discovered through an *in silico* screen based on cellular form prion-protein structure: correlation between antiprion activity and binding affinity. Antimicrob. Agents Chemother. **2009**, *53*, 765-771.

[96] Kimura, T.; Hosokawa-Muto, J.; Asami, K.; Murai, T. Kuwata, K. Synthesis of 9-substituted 2,3,4,9-tetrahydro-1H-carbazole derivatives and evaluation of their anti-prion activity in TSE-infected cells. *Eur. J. Med. Chem.* **2011**, *46*, 5675-5679.

[97] Ishibashi, D.; Nakagaki, T.; Ishikawa, T.; Atarashi, R.; Watanabe, K.; Cruz, F.A.; Hamada, T.; Nishida, N. Structure-based drug discovery for prion disease using a novel binding simulation. *EBioMedicine*, **2016**, *9*, 238-249.

[98] Caughey, B.; Raymond, L.D.; Raymond, G.J.; Maxson, L.; Silveira, J.; Baron, G.S. Inhibition of protease-resistant prion protein accumulation in vitro by curcumin. *J. Virol.* **2003**, *77*, 5499-5502.

[99] Hafner-Bratkovic, I.; Gaspersic, J.; Smid, M.L.; Bresjanac, M.; Jerala, R. Curcumin binds to the alpha-helical intermediate and to the amyloid form of prion protein – a new mechanism for the inhibition of PrP^{Sc} accumulation. *J. Neurochem.* **2008**, *104*, 1553-1564.

[100] Zanyatkin, I.; Stroylova, Y.; Tishina, S.; Stroylov, V.; Melnikova, A.; Haertle, T.; Muronetz, V. Inhibition of prion propagation by 3,4-dimethoxycynnamic acid. *Phytoter. Res.* **2017**, *31*, 1046-1055.

[101] Tatzelt, J.; Prusiner, S.B.; Welch, W.J. Chemical chaperones interfere with the formation of scrapie prion protein. *EMBO J.*, 1996, 15, 6363-6373.

[102] Prior, M.; Lehmann, S.; Sy, M.S.; Molloy, B.; McMahon, H.E. Cyclodextrins inhibit replication of scrapie prion protein in cell cultures. *J. Virol*, **2007**, *81*, 11195-11207.

[103] Bach, S.; Talarek, N.; Andrieu, T:; Vierfrond, J.M.; Mettey, Y.; Galons, H.; Dormont, D.; Meijer, L.; Cullin, C.; Blondel, M. Isolation of drugs active against mammalian prions using a yeast-based screening assay. *Nature Biotechnology*, **2003**, *21*, 1075-1081.

[104] Bach, S.; Tribouillard, D.; Talarek, N.; Desban, N.; Gug, F.; Galons, H.; Blondel, M. A yeast-based assay to isolate drugs active against mammalian prions. *Methods*, **2006**, *39*, 72-77.

[105] Tribouillard-Tanvier, D.; Béringue, V.; Desban N.; Gug, F.; Bach, S.; Voisset, C.; Galons, H.; Laude, H.; Vilette, D.; Blondel, M. Antihypertensive drug guanabenz is active in vivo against both yeast and mammalian prions. *PLoS One*, **2008**, *3*, e1981.

[106] Tribouillard-Tanvier, D.; Dos Reis, S.; Gug, F.; Voisset, C.; Béringue, V.; Sabate, R.; Kikovska, E.; Talarek, N.; Bach, S.; Huang, C.; Desban, N.; Saupe, S.J.; Supattapone, S.; Thuret, J.Y.; Chédin, S.; Vilette, D.; Galons, H.; Sanyal, S.; Blondel, M. Protein folding activity of ribosomal RNA is a selective target of two unrelated antiprion drugs. *PLoS One*, **2008**, *3*, e2174.

[107] Banerjee, D.; Sanyal, S. Protein folding activity of the ribosome (PFAR) – A target for antiprion compounds. *Viruses*, **2014**, *6*, 3907-3924.

[108] Pang, Y.; Kurella, S.; Voisset, C.; Samanta, D.; Banerjee, D.; Shabe, A.; Das Gupta, C.; Galons, H.; Blondel, M.; Sanyal, S. The antiprion compound 6-aminophenantridine inhibits the protein folding activity

of the ribosome by direct competition. *J. Biol. Chem.*, **2013**, *288*, 19081-19089.

[109] Banerjee, D.; Vovusha, H.; Pang, Y.; Oumata, N.; Sanyal, S. Spectroscopic and DFT studies on 6-aminophenanthridine and its derivatives provide insight in their activity towards ribosomal RNA. *Biochimie*, **2014**, *97*, 194-199.

[110] Oumata, N.; Nguyen, P.; Beringue, V.; Soubigou, F.; Pang, Y.; Desban, N.; Massacrier, C.; Morel, Y.; Paturel, C.; Contesse, M.A.; Bouaziz, S.; Sanyal, S.; Galons, H.; Blondel, M.; Voisset, C. The toll-like receptor agonist imiquimod is active against prions. *PLoS One*, **2013**, *8*, e72112.

[111] Nguyen, P.; Oumata, N.; Soubigou, F.; Evrard, J.; Desban, N.; Lemoine, P.; Bouaziz, S.; Blondel, M.; Voisset, C. Evaluation of the antiprion activity of 6-aminophenanthridines and related heterocycles. *Eur. J. Med. Chem.* **2014**, *82*, 363-371.

[112] Silber, B.M;, Gever, J.R.; Li, Z.; Gallardo-Godoy, A.; Renslo, A.R.; Widjaja, K.; Irwin, J.J.; Rao, S.; Jacobson, M.P.; Ghaemmaghami,, S.; Prusiner, S.B. Antiprion compounds that reduce PrP^{Sc} levels in dividing and stationary-phase cells. *Bioorg.Med. Chem.,* **2013**, *21*, 7999-8012

[113] Li, Z; Rao, S.; Gever, J.R.; Widjaja, K.; Prusiner, S.B.; Silber, B.M. Towards optimization of arylamides as novel, potent and brain-penetrant antiprion lead compounds. *ACS Med. Chem.Lett.,* **2013**, *4*, 647-650.

[114] Lu, D.; Giles, K.; Li, Z.; Rao, S.; Dolghih, E.; Gever, J.R.; Geva, M.; Elepano, M.L.; Oehler, A.; Bryant, C.; Renslo, A.R.; Jacobson, M.P.; DeAmond, S.J.; Silber, B.M.; Prusiner, S.B. Biaryl amides and hydrazones as therapeutics for prion disease in transgenic mice. *J. Pharmacol. Exp. Ther.*, **2013**, *347*, 325-338.

[115] Giles, K.; Berry, D.B.; Condello, C.; Dugger, B.N.; Li, Z.; Oehler, A.; Bhardway, S.; Elepano, M.; Guan, S.; Silber, M.; Olson, S.H.; Prusiner, S.B. Optimization of arylamides that extend survival in prion-infected mice. *J. Pharmacol. Exp. Ther.*, **2016**, *358*, 537-547.

[116] Thompson, M.J.; Borsenberger, V.; Louth, J.C.; Judd, K.E.; Chen, B. Design, synthesis and structure-activity relationship of indole-3-glyoxylamide libraries possessing highly potent activity in a cell line model of prion disease. *J. Med. Chem.*, **2009**, *52*, 7503-7511.

[117] Thompson, M.J.; Louth, J.C.; Ferrara, S.; Sorrell, F.J.; Irving, B.J.; Cochrane, E.J.; Meijer, A.J., Chen, B. Structure-activity relationship refinement and further assessment of indole-3-glyoxylamides as a lead series against prion disease. *ChemMedChem,* **2011**, *6*, 115-130.

[118] Bertsch, U.; Winklhofer, K.F.; Hirschberger, T.; Bieschke, J.; Weber, P.; Hartl, F.U.; Tavan, P.; Tatzelt, J.; Kretzschmar, H.A.; Giese, A. Systematic identification of antiprion drugs by high-throughput screening based on scanning for intensely fluorescent targets. *J. Virol.,* **2005**, *79*, 7785-7791.

[119] Kawasaki, Y.; Kawagoe, K.; Chen, C.; Teruya, K.; Sakasegawa, Y.; Doh-ura, K. Orally administered amyloidophilic compound is effective in prolonging the incubation period of animals cerebrally infected with prion diseases in a prion strain-dependent manner. *J.Virol.*, **2007**, *81*, 12889-12898.

[120] Zaccagnini, L.; Brogi, S.; Brindisi, M.; Gemma, S.; Chemi, G.; Legname, G.; Campiani, G.; Butini, S. Identification of novel fluorescent probes preventing PrP^{Sc} replication in prion diseases. *Eur. J. Med. Chem.*, **2017**, *127*, 859-873.

[121] Geissen, M., Leidel, F.; Eiden, M., Hirschberger, T., Fast, C., Bertsch, U., Tavan, P., Giese, A., Kretzschmar, H., Schatzl, H.M., Groschup, M.H. From high-throughput cell culture screening to mouse model: identification of new inhibitor classes against prion disease. *ChemMedChem*, **2011**, *6*, 1928-1937.

[122] Kimata, A.; Nakagawa, H.; Ohyama, R.; Fukuuchi, T.; Ohta, S.; Suzuki, T.; Miyata, N. New series of antiprion compounds: pyrazolone derivatives have the potent activity of inhibiting protease-resistant prion protein accumulation. *J.Med.Chem.,* **2007**, *50*, 5053-5057.

[123] Wagner, J.; Ryazanov, S.; Leonov, A.; Levin, J.; Shi, S.; Schmidt, F.; Prix, C.; Pan-Montojo, F.; Bertsch, U.; Mitteregger-Kretzschmar, G.; Geissen, M.; Eiden, M.; Leidel, F.; Hirschberger, T.; Deeg, A.A.; Krauth, J.J.; Zinth, W.; Tavan, P.; Pilger, J.; Zweckstetter, M.; Frank, T.; Bähr, M.; Weishaupt, J.H.; Uhr, M.; Urlaub, H.; Teichmann, U.; Samwer, M.; Bötzel, K.; Groschup, M.; Kretzschmar, H.; Griesinger, C.; Giese, A. Anle 138b: a novel oligomer-modulator for disease-modifying therapy of neurodegenerative diseases such as prion and Parkinson's disease. *Acta Neuropathol.*, **2013**, *125*, 795-813.

[124] Stanton, J.B.; Schneider, D.A.; Dinkel, K.D.; Balmer, B.F.; Baszler, T.V.; Mathison, B.A.; Boykin, D.W.; Kumar. A. Discover of a novel, monocationic, small-molecule inhibitor of scrapie prion accumulation in cultured sheep microglia and Rov cells. *PLoS One* **2012**, *7*, e51173.

[125] Dinkel, K.D.; Stanton, J.B.; Boykin, D.W.; Stephens, C.E.; Madsen-Bouterse, S.A.; Schneider, D.A. Antiprion activity of DB-772 and related monothiophene- and furan based analogs in a persistently infected ovine microglia culture system. *Antimicrob. Agents Chemother.* **2016**, *60*, 5467-5482.

[126] Li, Z.; Gever, J.R.; Rao, S.; Widjaja, K.; Prusiner, S.B.; Silber, B.M. Discovery and preliminary structure-activity relationship of arylpiperazines as novel, brain-penetrant anti-prion compounds. *ACS Med. Chem. Lett.*, **2013**, *4*, 397-401.

[127] Leidel, F.; Eiden, M.; Geissen, M.; Hirschberger, T.; Tavan, P.; Giese, A.; Kretzschmar, H.A.; Schätzl, H.; Groschup, M.H. Piperazine derivatives inhibit PrP/PrP^{res} propagation in vitro and in vivo. *Biochem. Biophys. Res. Commun*. **2014**, *445*, 23-29.

[128] Ferreira, N.C.; Marques, I.A.; Conceição,W.A.; Macedo, B.; Machado, C.S.; Mascarello, A.; Chiaradia-Delatorre L.D.; Yunes, R.A.; Nunes, R.J.; Hughson, A.G.; Raymond, L.D.; Pascutti, P.G.; Caughey, B.; Cordeiro, Y. Anti-prion activity of a panel of aromatic chemical compounds: *in vitro* and *in silico* approaches. *PLoS One*, **2014**, *9*, e84531.

[129] Ayrolles-Torro, A.; Imberdis, T.; Torrent, J.; Toupet, K.; Baskakov, I.V.; Poncet-Montange, G.; Grégoire, C.; Roquet-Baneres, F.; Lehmann, S.; Rognan, D.; Pugnière, M.; Verdier, J.M.; Perrier, V. Oligomeric-induced activity by thienyl pyrimidine compounds traps prion infectivity. *J. Neurosci.* **2011**, *31*, 14882-14892.

[130] Simoneau, S.; Rezaei, H.; Salès, N.; Kaiser-Schulz, G.; Lefebvre-Roque, M.; Vidal, C.; Fournier, J.G.; Comte, J.; Wopfner, F.; Grosclaude, J.; Schätzl, H.; Lasmézas, C.I. In vitro and in vivo neurotoxicity of prion protein oligomers. *PLoS Pathog.* **2007**, *3*, e125.

[131] Tagliavini, F.; McArthur, R.A.; Canciani, B.; Giaccone, G.; Porro, M.; Bugiani, M.; Lievens, P.M.J.; Bugiani, O.; Peri, E.; Dall'Ara, P.; Rocchi, M.; Poli, G.; Forloni, G.; Bandiera, T.; Varasi, M.; Suarato, A.; Cassutti, P.; Cervini, M.A;, Lansen, J.; Salmona, M.; Post, C. Effectiveness of anthracycline against experimental prion disease in Syrian hamsters. *Science*, **1997**, *276*, 1119-1122.

[132] Forloni, G.; Iussich, S.; Awan, T.; Colombo, L.; Angeretti, N.; Girola, L.; Bertani, I.; Poli, G.; Caramelli, M.; Bruzzone, M. G.; Farina, L.; Limido, L.; Rossi, G.; Giaccone, G.; Ironside, J.W.; Bugiani, O.; Salmona, M.; Tagliavini, F. Tetracyclines affect prion infectivity. *Proc. Natl. Acad. Sci. USA*, **2002**, *99*, 10849-10854.

[133] Tagliavini, F.; Forloni, G.; Colombo, L.; Rossi, G.; Girola, L.; Canciani, B.; Angeretti, N.; Giampaolo, L.; Peressini, E.; Awan, T.; De Gioia, L.; Ragg, E.; Bugiani, O.; Salmona, M. Tetracycline aggects abnormal properties of synthetic PrP peptides and PrP^{Sc} *in vitro*. *J. Mol. Biol.*, **2000**, *300*, 1309-1322.

[134] Halk, S.; Marcon, G.; Mallet, A.; Tettamanti, M.; Welaratne, A.; Giaccone, G.; Azimi, S.; Pietrini, V.; Fabreguettes, J.R.; Imperiale, D.; Cesaro, P.; Buffa, C.; Aucan, C.; Lucca, U.; Peckeu, L.; Suardi, S.; Tranchant, C.; Zerr, I.; Houillier, C.; Redaelli, V.; Vespignani, H.; Campanella, A.; Sellal, F.; Krasniaski, A.; Seilhean, D.; Heinemann, U.; Sedel, F.; Canovi, M.; Gobbi, M.; Di Fede, G.; Laplanche, J.L.; Pocchiari, M.; Salmona, M.; Forloni, G.; Brandel, J.P.; Tagliavini, F. Doxycycline in Creutzfeldt-Jakob disease: a phase 2, randomized, double-blind, placebo-controlled trial. *Lancet Neurol.*, **2014**, *13*, 150-158.

[135] Charvériat, M.; Reboul, M.; Wang, Q.; Picoli, C.; Lenuzza, N.; Montagnac, A.; Nhiri, N,; Jacquet, E.; Guéritte, F.; Lallemand, J.Y.; Deslys, J.P.; Mouthon, F. New inhibitors of prion replication that target the amyloid precursor. *J. Gen. Virol.*, **2009**, *90*, 1294-1301.

[136] Marella, M.; Lehmann, S.; Grassi, J.; Chabry, J. Filipin prevents pathological prion protein accumulation by reducing endocytosis and inducing cellular PrP release. *J. Biol. Chem.* **2002**, *277*, 25457-25464.

[137] Xi, Y.G.; Ingrosso, L.; Ladogana, A.; Masullo, C.; Pocchiari, M. Amphotericin B treatment dissociates in vivo replication of the scrapie agent from PrP accumulation. *Nature*, **1992**, *356*, 598-601.

[138] Adjou, K.T.; Demaimay, R.; Deslys, J.P.; Lasmézas, C.I.; Beringue, V.; Demart, S.; Lamoury, F.; Seman, M.; Dormont, D. MS-8209, a water-soluble amphotericin B derivative, affects both scrapie agent replication and PrPres accumulation in Syrian hamster scrapie. *J. Gen. Virol.*, **1999**, *80*, 179-185.

[139] Vey, M.; Pilkuhn, S.; Wille, H.; Nixon, R.; DeAmond, S.J.; Smart, E.J.; Anderson, R.G.; Taraboulos, A.; Prusiner, S.B. Subcellular colocalization of the cellular and scrapie prion proteins in caveolae-like membranous domains. *Proc. Natl. Acad. Sci. USA*, **1996**, *93*, 14945-14949.

[140] Mangé, A.; Nishida, N.; Milhavet, O.; McMahon, H.E.; Casanova, D.; Lehmann, S. Amphotericin B inhibits the generation of the scrapie isoform of the prion protein in infected cultures. *J. Virol.*, **2000**, *74*, 3135-3140.

[141] Taraboulos, A.M.; Scott, M.; Semenov, A.; Avrahami. D.; Laszlo, L.; Prusiner, S.B. Cholesterol depletion and modification of COOH-terminal targeting sequence of the prion protein inhibits formation of the scrapie isoform. *J. Cell Biol.*, **1995**, *129*, 121-132.

[142] Bate, C.; Salmona, M.; Diomede, L.; Williams, A. Squalestatin cures prion-infected neurons and protects against prion neurotoxicity. *J. Biol. Chem.*, **2004**, *270*, 14983-14990.

[143] Outram, G.W.; Dickinson, A.G.; Fraser, H. Reduced susceptibility to scrapie in mice after steroid administration. *Nature*, **1974**, *249*, 855-856.

[144] Kocisko, D.A.; Baron, G.S.; Rubenstein, R.; Chen. J.; Kuizon, S.; Caughey, B. New inhibitors of scrapie-associated prion protein formation in a library of 2,000 drugs and natural products. *J. Virol.*, **2003**, *77*, 10288-10294.

[145] Gilch, S; Bach, C.; Lutzny, G.; Vorberg, I.; Schätzl, H.M. Inhibition of cholesterol recycling impairs cellular PrPSc propagation. *Cell Mol. Life Sci.*, **2009**, *66*, 3979-3991.

[146] Heiseke, A; Aguib, Y.; M.; Schätzl, H.M. Autophagy, prion infection and their mutual interactions. *Curr. Issues Mol. Biol.,* **2010**, *12*, 87-89.

[147] Karapetyan, Y.E.; Sferrazza, G.F.; Zhou, M.; Ottenberg, G.; Spicer, T.; Chase, P.; Fallahi, M.; Hodder, P.; Weissmann, C.; Lasmézas, C.I. Unique drug screening approach for prion diseases identifies tacrolimus and astemizole as antiprion agents. *Proc. Natl. Acad. Sci. USA*, **2013**, *110*, 7044-7049.

[148] Marzo, L.; Marijanovic, Z.; Browman, D.; Chamoun, Z.; Caputo, A.; Zurzolo, C. 4-hydroxytamoxifen leads to PrP^{Sc} clearance by conveying both PrPC and PrP^{Sc} to lysosomes independently of autophagy. *J. Cell. Sci.* **2013**, *126*, 1345-1354.

[149] Perovic, S.; Schröder, H.C.; Pergande, G.; Ushijima, H.; Müller, W.E.G. Effect of flupirtine on Bcl-2 and glutathione level in neuronal cells treated in vitro with the prion protein fragment (PrP106-126). *Exp. Neurol.* **1997**, *147*, 518-524.

[150] Otto, M.; Cepek, L.; Ratzka, P.; Doehlinger, S.; Boekhoff, I.; Wiltfang, J.; Irle, E.; Pergande, G.; Ellers-Lenz, B.; Windl, O.; Kretzschmar, H.A.; Poser, S.; Prange, H. Efficacy of flupirtine on cognitive function in patients with CJD: a double-blind study. *Neurology*, **2004**, *62*, 714-718.

[151] Nishizawa, K.; Oguma, A.; Kawata, M.; Sakasegawa, Y.; Teruya, K.; Doh-ura, K. Efficacy and mechanism of a glycoside compound inhibiting abnormal prion protein formation in prion-infected cells: implication of interferon and phosphodiesterase 4D-interacting protein. *J. Virol*, **2014**, *88*, 4083-4099.

[152] Touil, F., Pratt., S., Mutter, R.; Chen, B. Screening a library of potential prion therapeutics against cellular prion proteins and insights into their mode of biological activities by surface plasmon resonance. *J. Pharm. Biomed. Anal.* **2006**, *40*, 822-832.

[153] Kovačević, S.; Karadžić, M.; Podunavac-Kuzmanović, S.; Jevrić, L. Binding affinity toward human prion protein of some anti-prion compounds. – Assessment based on QSAR modeling, molecular docking and non-parametric ranking. *Eur. J. Pharm. Sci.* **2018**, *111*, 215-225.

[154] Bolognesi, M.L.; Legname, G. Approaches for discovering anti-prion compounds: lessons learned and challenges ahead. *Expert Opin. Drug Discov.*, **2015**, *10*, 389-397.

[155] Nakajima, M.; Yamada, T.; Kusuhara, T.; Furukawa, H.; Takahashi, M.; Yamauchi, A.; Kataoka, Y. Results of quinacrine administration to patients with Creutzfeldt-Jakob disease. *Dement. Geriatr. Cogn. Disord.* **2004**, *17*, 158-163.

[156] Barreca, M.L.; Iraci, N.; Biggi, S. ; Cecchetti, V.; Biasini, E. Pharmacological agents targeting the cellular prion protein. *Pathogens*, **2018**, *7*, 27.

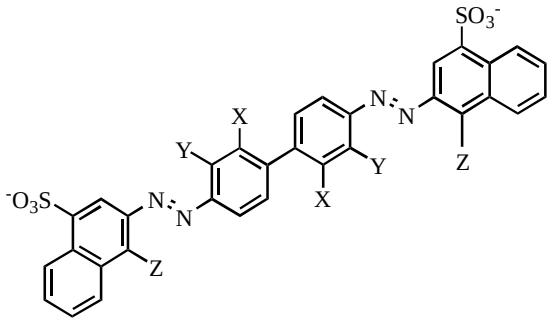

Congo red X=Y=H, Z=NH_2
2a X=Me,Y=H, Z=NH_2
2b X=H, Y=Me, Z=NH_2
2c X=H, Y=OMe, Z=NH_2
2d X=H, Y=Cl, Z=NH_2
2e X=Y=H, Z=$NHCOCH_3$
2f X=Y=H, Z=OH
2g X=H, Y=OMe, Z=OH
2h X=H, Y=COOH, Z=NH_2

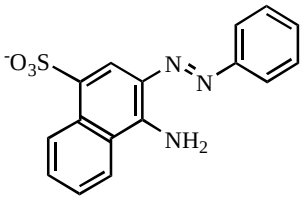

1

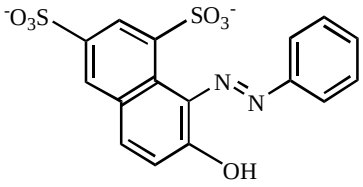

Orange G

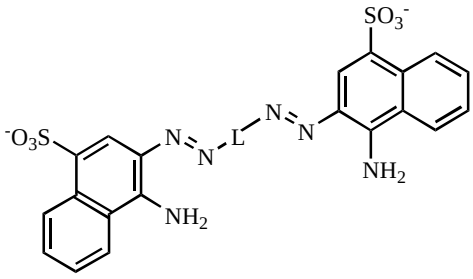

3a L=

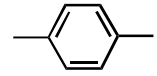

3b L=

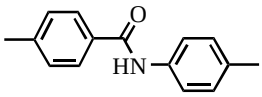

3c L=

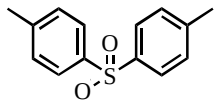

3d L=

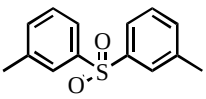

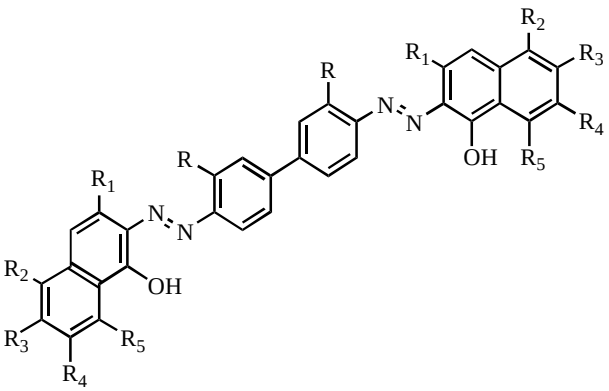

4a R=OMe, R_1=SO_3^-, R_2=R_4=R_5=H, R_3=NH_2
4b R=Me, R_1=R_3=SO_3^-, R_2=R_4=H, R_5=NH_2
4c R=OMe, R_1=R_3=H, R_2=R_4=SO_3^-, R_5=NH_2

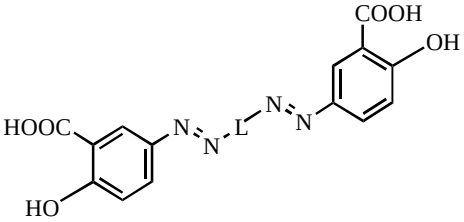

Chrysamine G **L=**

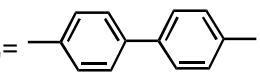

5a **L=**

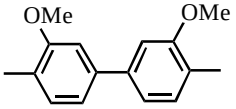

5b **L=**

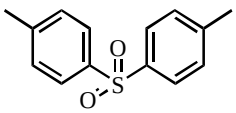

5c **L=**

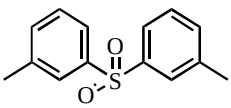

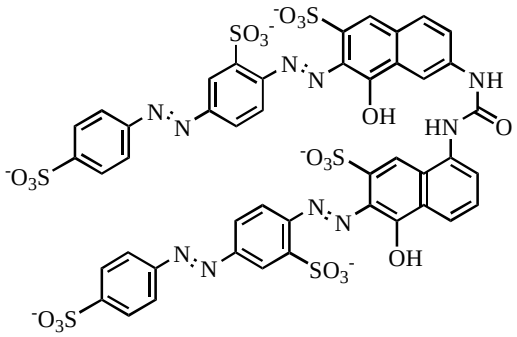

Sirius red

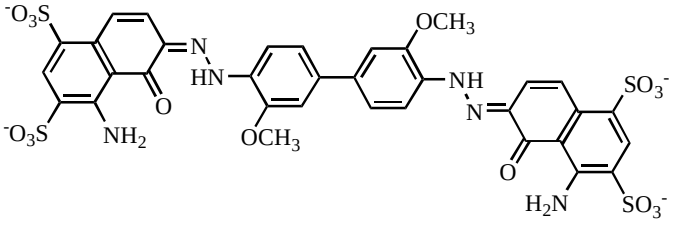

Chicago Sky Blue 6B

Figure 1. Congo-Red related azo dyes

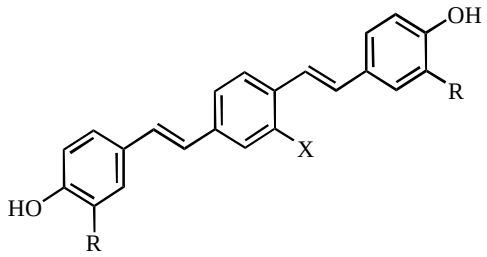

BSB X=Br, R=COOH
X-34 X=H, R=COOH
6 X=R=H

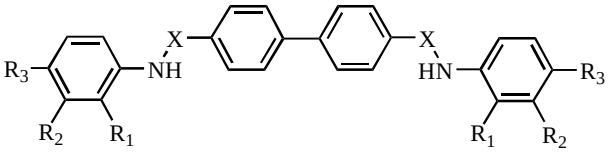

7a X=CO, R_1=OH, R_2=H, R_3=COOMe
7b X=SO_2, R_1=OH, R_2=H, R_3=COOMe
7c X=CO, R_1=H, R_2=OMe, R_3=COOMe
7d X=CO, R_1=H, R_2=COOMe, R_3=OH
7e R_1=H, R_2=OH, R_3=COOMe
7f R_1=OH, R_2=H, R_3=H
7g R_1=H, R_2=OMe, R_3=COOH
7h R_1=OH, R_2=H, R_3=NO_2

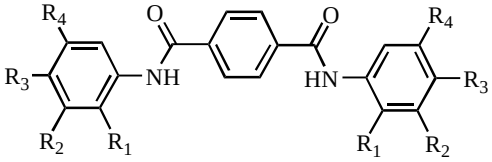

8a R_1=R_3=H, R_2=R_4=COOMe
8b R_1=OH, R_2=R_4=H, R_3=COOMe

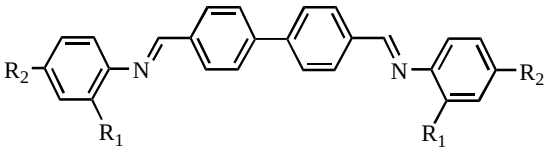

9a R_1=OH, R_2=COOMe
9b R_1=H, R_2=OH

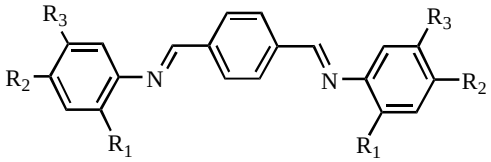

10a R_1=R_3=H, R_2=CN
10b R_1=OCF_3, R_2=H, R_3=COOMe

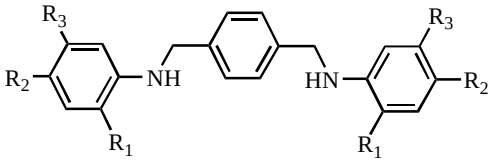

11a R_1=OMe, R_2=H, R_3=COOMe
11b R_1=OH, R_2=COOMe. R_3=H
11c R_1=OH, R_2=R_3=H
11d R_1=OCF_3, R_2=H, R_3=COOMe
11e R_1=OCF_3, R_2=H, R_3=COOH
11f R_1=OCF_3, R_2=H, R_3=$COO(CH_2)_3NMe_2$

Figure 2. Congo-Red related fluorescent ligands lacking of azo group

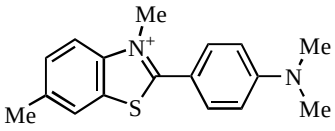

Thioflavin T

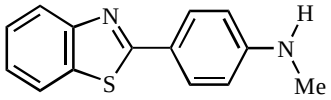

BTA-1

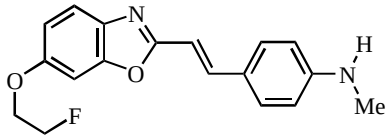

BF-168

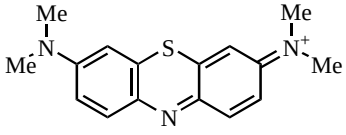

Methylene Blue

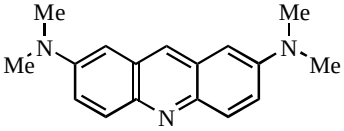

Acridine Orange

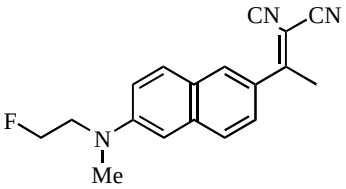

FDDNP

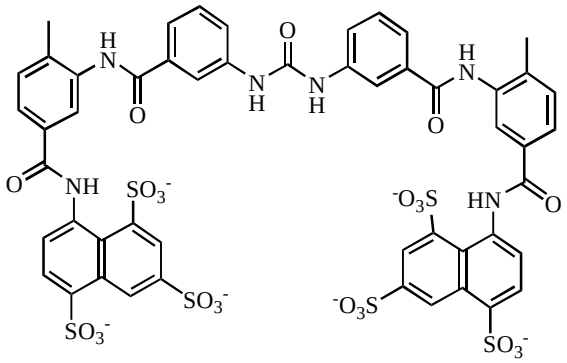

Suramin

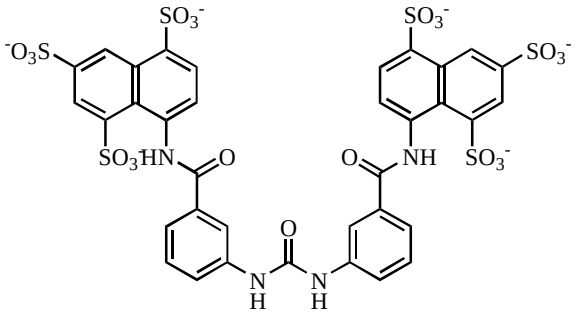

12

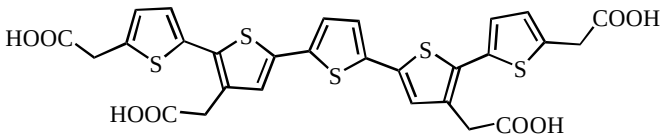

13

Figure 3. Miscellaneus fluorescent prion ligands

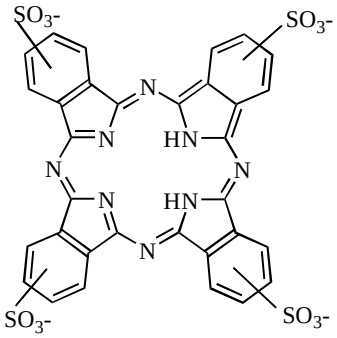

PcTS

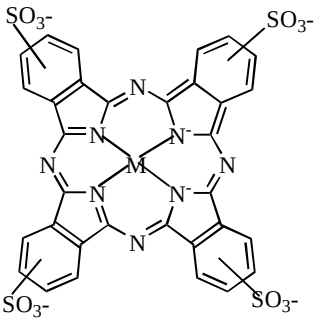

PcTS metal complexes

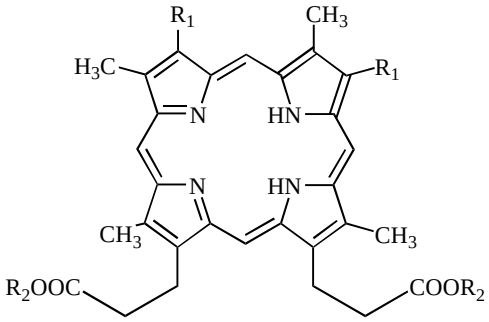

14a R_1=SO_3^-, R_2=H
14b R_1=SO_3^-, R_2=CH_3
14c R_1=CH_2CH_2OH, R_2=H

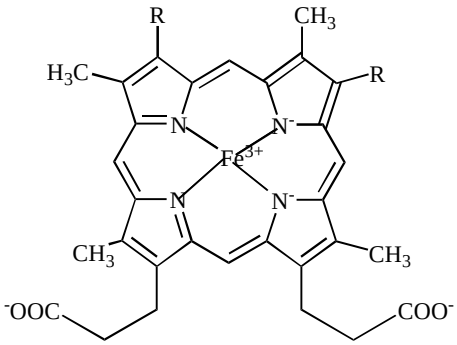

15a R=SO_3^-
15b
R=CH_2CH_2OH

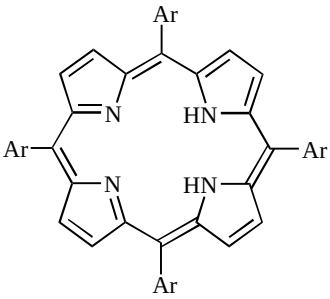

16a Ar=*p*-(SO_3^-)Ph
16b Ar=*p*-(COOH)Ph
16c Ar=*p*-(NMe_3^+)Ph
16d Ar=4-pyridyl
16e Ar=N^+-Me-4-pyridyl
16f Ar=N^+-Me-3-pyridyl
16g Ar=N^+-Me-2-pyridyl

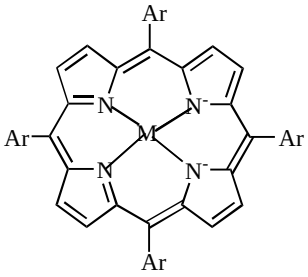

17a Ar=*p*-(SO_3^-)Ph, M=Fe^{3+}
17b Ar=*p*-(SO_3^-)Ph, M=Mn^{3+}
17c Ar=*p*-(COOH)Ph, M=Fe^{3+}
17d Ar=*p*-(NMe_3^+)Ph, M=Fe^{3+}
17e Ar=N^+-Me-4-pyridyl, M=Fe^{3+}
17f Ar=N^+-Me-4-pyridyl, M=Cu^{2+}
17g Ar=N^+-Me-4-pyridyl, M=Ni^{2+}
17h Ar=N^+-Me-4-pyridyl, M=Zn^{2+}

Figure 4. Porphyins and phthalocyanines

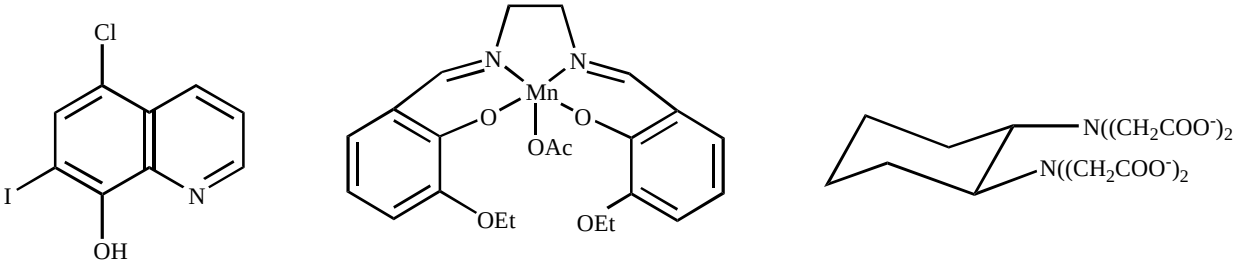

Clioquinol **EUK 189** **CDTA**

Figure 5. Metal ion chelators and chelates.

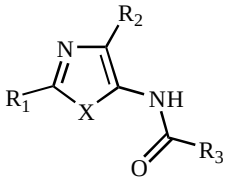

18a R_1=3-pyridyl, R_2=SPh, R_3=2-furyl, X=S
18b R_1=R_2=Ph, R_3=CF_3, X=S
18c R_1=R_2=Ph, R_3=CF_3, X=O
18d R_1=R_2=Ph, R_3=CMe_3, X=O
18e R_1=R_2=Ph, R_3=2-CF_3-Ph, X=O
18f R_1=R_2=Ph, R_3=benzothiazol-2-yl, X=S

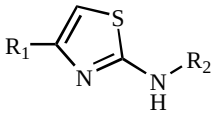

19a R_1=3,4-di(OH)Ph, R_2=6-Me-2-pyridyl
19b R_1=2,4-di(OH)Ph, R_2=6-Me-2-pyridyl
19c R_1=3,4-di(OH)Ph, R_2=2-pyridyl
19d R_1=3,4-di(OH)Ph, R_2=3-COOH-4-OH-Ph
19e R_1=3,4-di(OMe)Ph, R_2=6-Me-2-pyridyl
19f R_1=3,4-di(OMe)Ph, R_2=5-Me-2-pyridyl
19g R_1=4-MeOPh, R_2=4-Me-2-pyridyl
19h R_1=2-MeOPh, R_2=4-Me-2-pyridyl
19i R_1=3-Ph-oxazol-5-yl, R_2=5-OMe-2-pyridyl
19j R_1=3-Ph-oxazol-5-yl, R_2=4-OMe-2-pyridyl
19k R_1=3,4-di(OMe)Ph-NHCO, R_2=4-Me-2-pyridyl

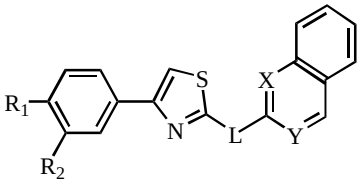

20a R_1=R_2=OMe, X=Y=CH, L=NH
20b R_1=R_2=OMe, X=N, Y=CH, L=NH
20c R_1=R_2=OMe, X=CH, Y=N; L=NH
20d R_1=OCF_3, R_2=H, X=CH, Y=N, L=NH
20e R_1=R_2=OMe, X=CH, Y=N, L=CONH
20f R_1=R_2=OMe, X=CH, Y=N, L=NHCO
20g R_1=R_2=OMe, X=CH, Y=N, L=NMe
20h R_1=R_2=OMe, X=CH, Y=N, L=NAc

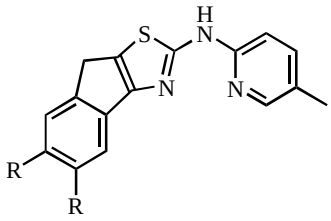

21a R=OMe
21b R=H

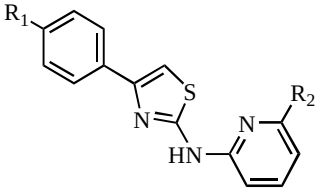

22a R_1=Ph, R_2=Me
22b R_1=3-pyridyl, R_2=Me
22c R_1=4-pyridyl, R_2=Me
22d R_1=morpholino, R_2=Me
22e R_1=Ph, R_2=NMe_2

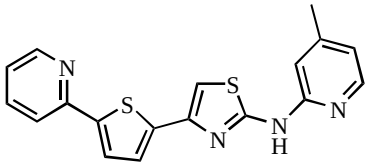

23

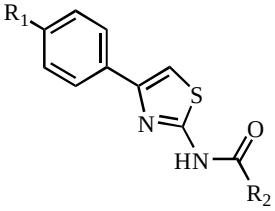

24a R_1=Ph, R_2=cyclopropyl
24b R_1=2-Me-3-pyridyl, R_2=cyclopropyl
24c R_1=4-NMe_2-3-pyridyl, R_2=cyclopropyl

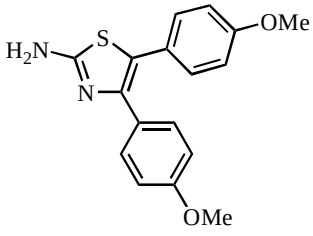

25

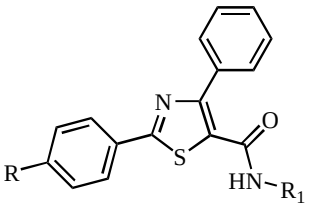

26a R=H, R_1=$(CH_2)_2NEt_2$
26b R=OMe, R_1=$(CH_2)_2NEt_2$
26c R=H, R_1=$(CH_2)_2NMe_2$
26d R=H, R_1=CH_2(2-furyl)
26e R=H, R_1=$(CH_2)_3NEt_2$
26f R=H, R_1=CH(Me)-$(CH_2)_2NEt_2$

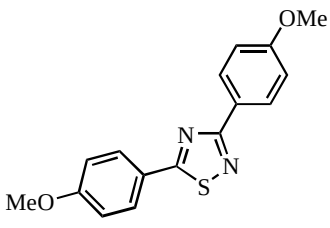

27

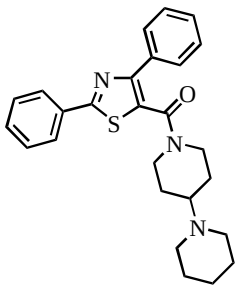

28

Figure 6. Aminothiazoles and related compounds.

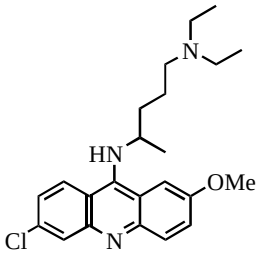

Quinacrine

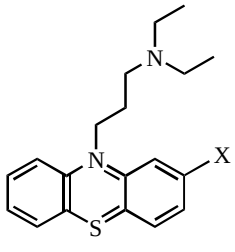

X=Cl Chlorpromazine
X=H Promazine
X=Ac Acepromazine

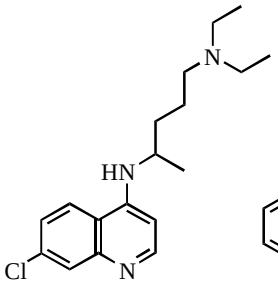

Chloroquine

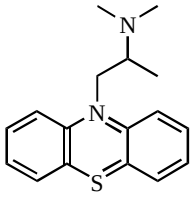

Promethazine

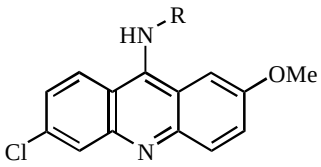

29a R=$(CH_2)_2CHMe_2$
29b R=$(CH_2)_4CH_3$
29c R=$(CH_2)_3OEt$
29d R=CH_2-(2-furyl)
29e R=p-MeO-benzyl

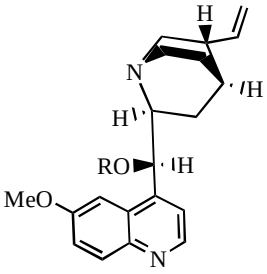

Quinine R=H
30 R=COOEt

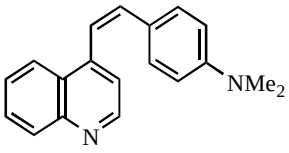

31

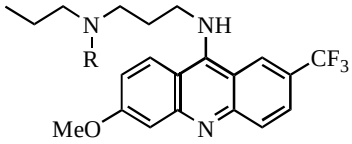

32a R=Pr
32b R=CH_2Ph

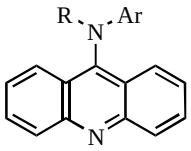

33a R=H, Ar=Ph
33b R=Me, Ar=Ph
33c R=H, Ar=*m*-NH_2-Ph
33d R=H, Ar=*m*-MeS-Ph

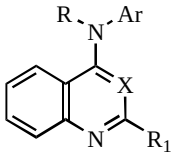

34a X=N, R=H, R_1=Ar=Ph
34b X=N, R=Me, R_1=Ar=Ph
34c X=CH, R=H, R_1=Me, Ar=Ph
34d X=CH, R=H, R_1=Me, Ar=m-MeOPh

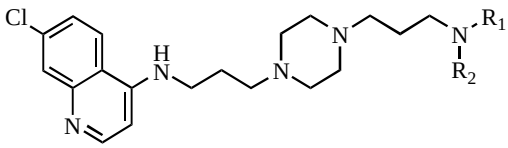

35a R_1=H, R_2=SO_2CH_3
35b R_1=H, R_2=$COCH_2NH_2$
35c R_1=H, R_2=SO_2Ph
35d R_1=H, R_2=COPh,
35e R_1=H, R_2=SO_2(2-thienyl)
35f R_1=H, R_2=CH_2(3-thienyl)
35g R_1=H, R_2=SO_2(*p*-MeOPh)
35h R_1=H, R_2=CH_2(*m*-PhOPh)
35i R_1=CH_2(cyclopropyl), R_2=β-naphthoyl
35j R_1=H, R_2=SO_2(5-NMe_2-1-naphthyl)
35k R_1=H, R_2=CO(4-quinolinyl)

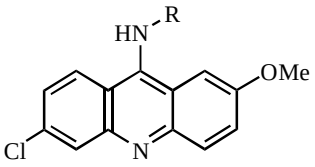

36a R=$(CH_2)_2NEt_2$

36b R= 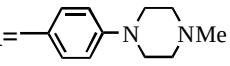

36c R= 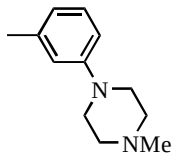

36d R= 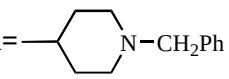

36e R= 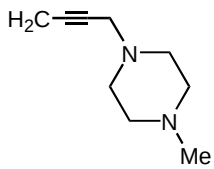

36f R=Ph

36g R=H

36h R= 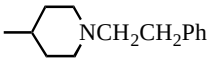

36i R= 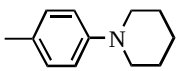

36j R= 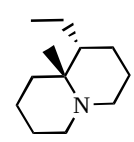

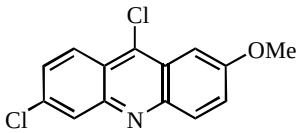

37

Figure 7. Acridines, quinolines, quinazolines and phenothiazines with a single pharmacophoric unity

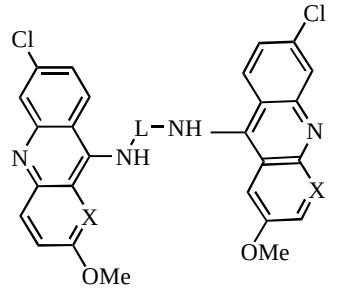

38a X=CH, L=$(CH_2)_8$
38b X=CH,
L=$(CH_2)_2O(CH_2)_2O(CH_2)_2$
38c X=CH, L=$(CH_2)_3NH(CH_2)_4$

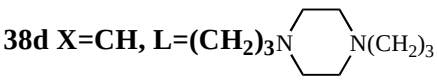

38d X=CH, L=$(CH_2)_3$

38e X=CH, L=(*S*)-$(CH_2)_3N(CH_2)_4$

COCH(Me)NHCOOCMe$_3$

38f X=N, L=$(CH_2)_3NH(CH_2)_4$

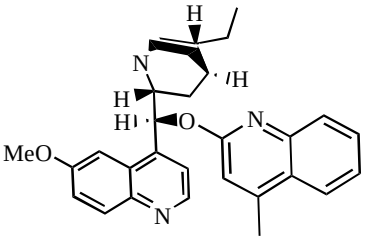

39

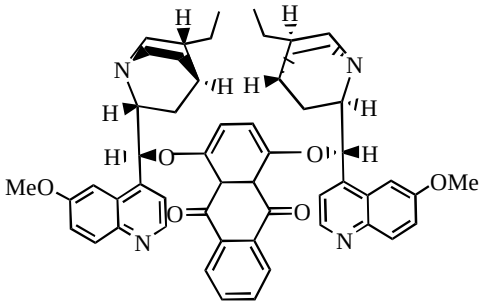

40

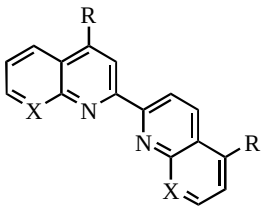

41a R=H, X=CH
41b R=H, X=N
41c R=COOH, X=CH

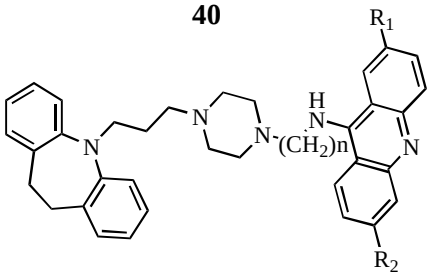

Quinpramine n=4, R_1=OMe, R_2=Cl
42 n=2, R_1=R_2=H

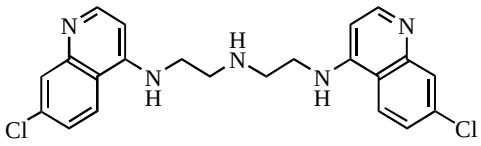

43

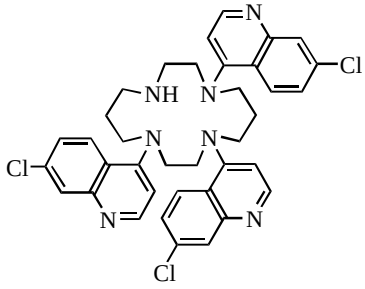

44

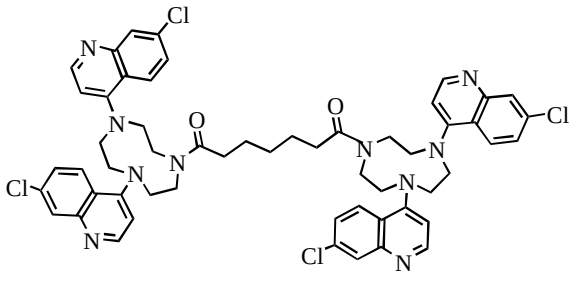

45

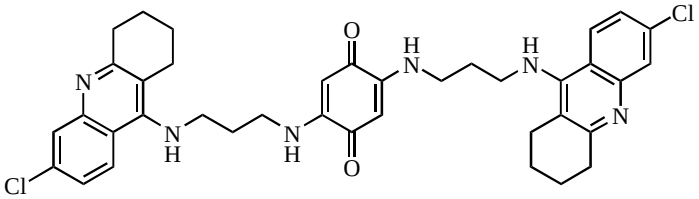

46

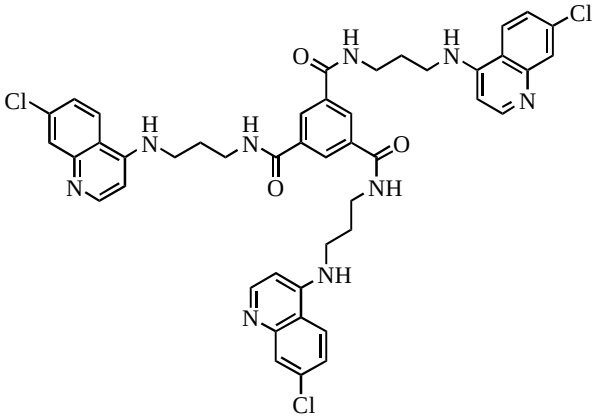

47

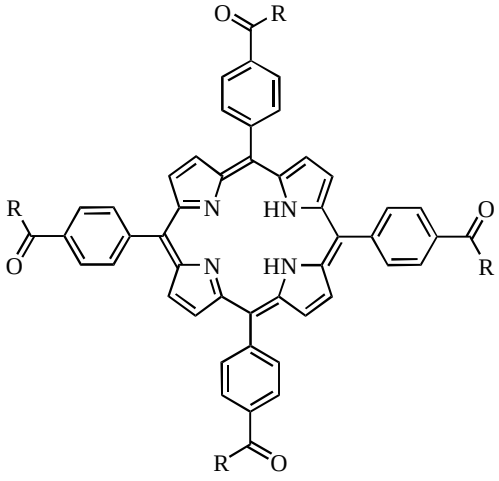

48
R=$NH(CH_2)_3NH$(7-Cl-4-quinolyl)

Figure 8. Polyvalent acridine and quinoline derivatives.

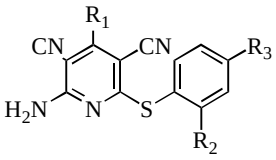

Cp-60 R_1=2-furyl, R_2=NH_2, R_3=H
49 R_1=Ph, R_2=H, R_3=Cl

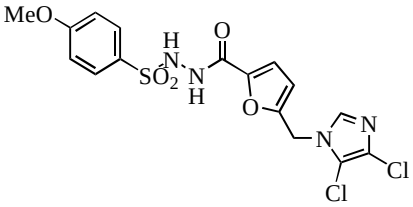

Cp-62

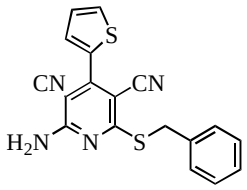

50

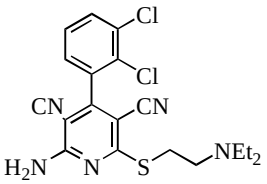

51

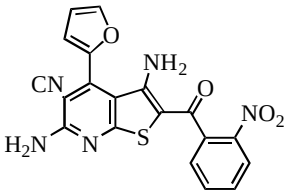

52

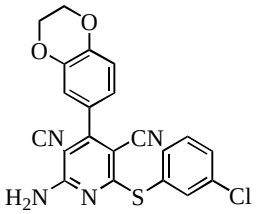

53

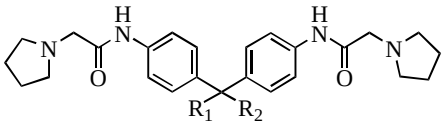

GN8 R_1=R_2=H
54a R_1=cycloheptyl, R_2=H
54b R_1=CF_3, R_2=*p*-FPh

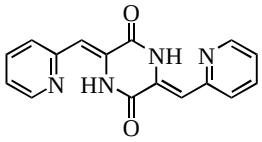

55

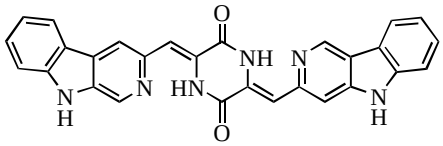

56

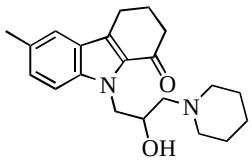

57

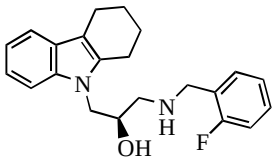

58

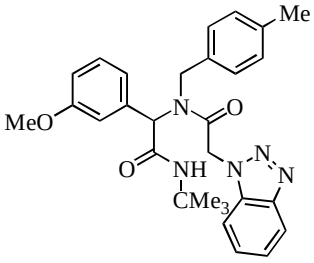

NPR-053

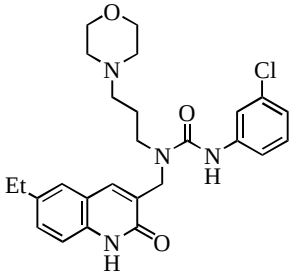

NPR-056

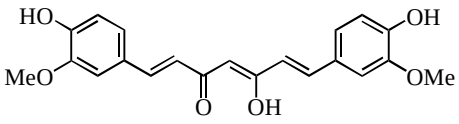

Curcumin

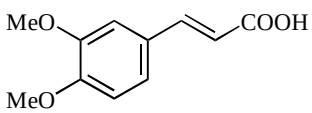

3,4-Dimethoxycynnamic acid

Figure 9. Compounds acting as chaperones towards the native prion protein.

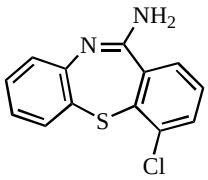

59

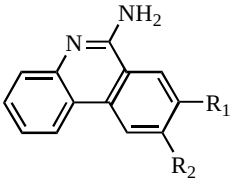

60a R_1=R_2=H
60b R_1=Cl, R_2=H
60c R_1=CF_3, R_2=H
60d R_1=H, R_2=F
60e R_1=N_3, R_2=H

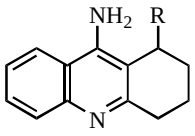

Tacrine R=H
Hydroxytacrine R=OH

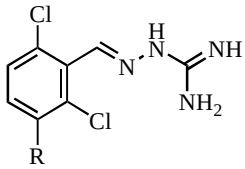

Guanabenz R=H
61 R=Cl

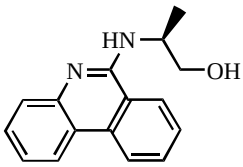

62

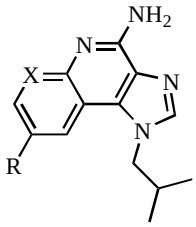

Imiquimod R=H, X=CH
63a R=Me, X=CH
63b R=Cl, X=CH
63c R=H, X=N

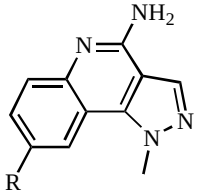

64a R=H
64b R=Cl

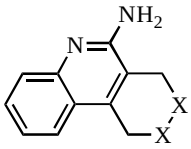

65a XX=CH_2CH_2
65b XX=CH=CH

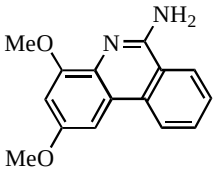

66

Figure 10. Inhibitors of the protein-folding activity of ribosomes.

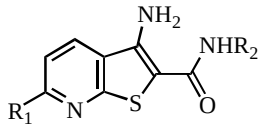

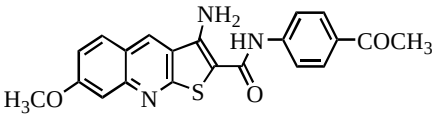

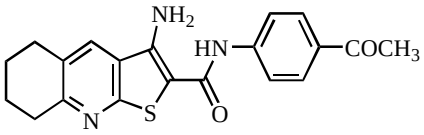

67a R_1=*p*-MeOPh, R_2=*p*-FPh
67b R_1=*p*-MeOPh, R_2=*p*-AcPh

68

69

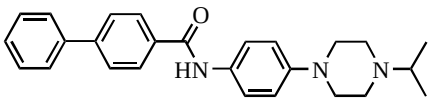

70

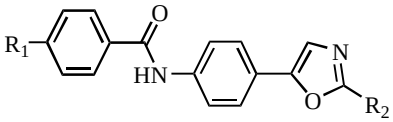

71a R_1=R_2=H
71b R_1=MeO, R_2=H
71c R_1=Cl, R_2=H
71d R_1=F, R_2=cyclopropyl
71e R_1=$MeOCH_2CH_2O$, R_2=cyclopropyl

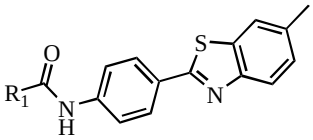

72a R_1=3-Me-2-furyl
72b R_1=3-furyl
72c R_1=3-Me-2-furyl

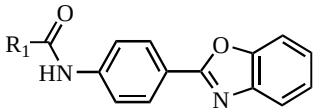

73a R_1=*p*-MeOPh
73b R_1=3-furyl

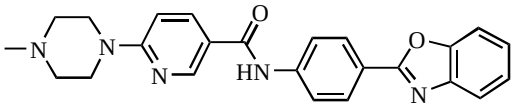

74

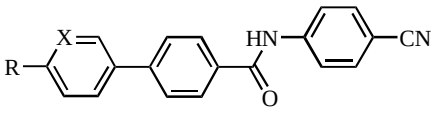

75a X=CH, R=H
75b X=N, R=H
75c X=N, R=OCH_2CH_2OMe

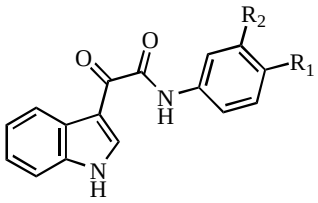

76a R_1=H, R_2=Cl
76b R_1=OMe, R_2=H
76c R_1=pyrazol-1-yl, R_2=H

Figure 11. *N*-(Aryl or hetaryl)amides

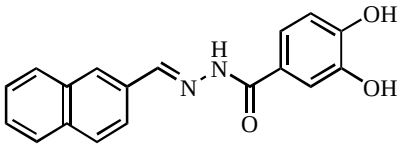

77

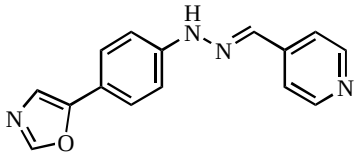

Compound B

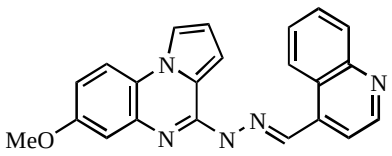

78

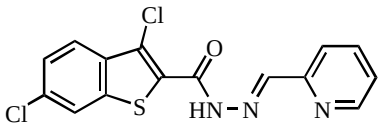

79

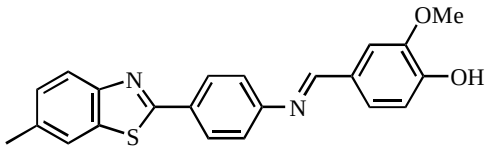

80

Figure 12. Hydrazones and azomethinic compounds.

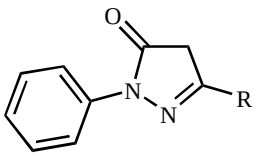

81 R=*p*-NO_2-Ph
Edaravone R=Me

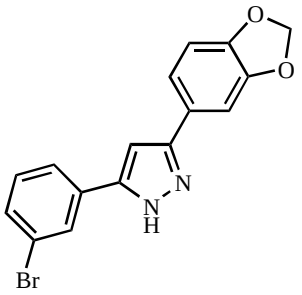

Anle 138b

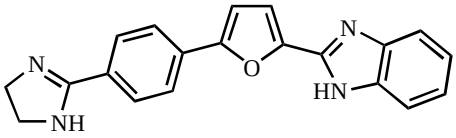

DB772

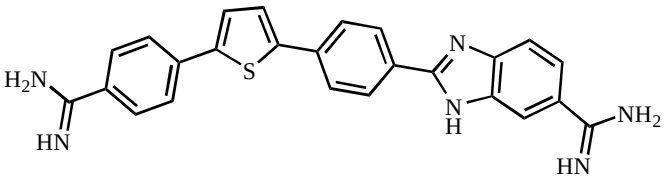

82

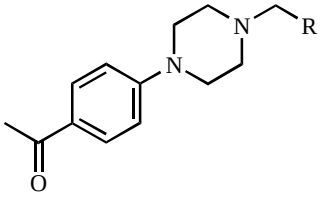

83a R=Ph
83b R=Et

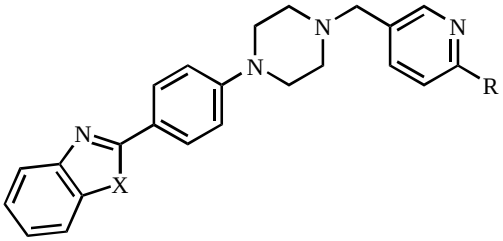

84a X=O, R=H
84b X=S, R=H
84c X=O, R=F

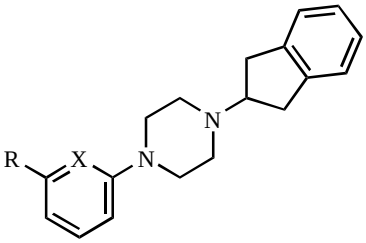

85a X=N, R=H
85b X=CH, R=Cl

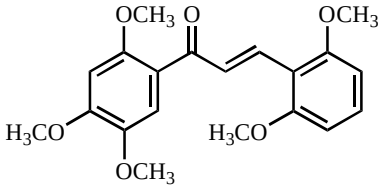

86

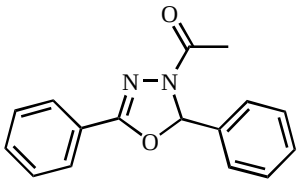

87

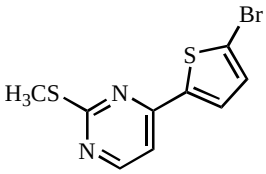

88

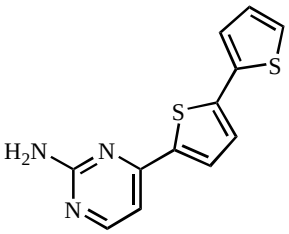

89

Figure 13. Simple aromatic and heterocyclic molecules tested for antiprion activity.

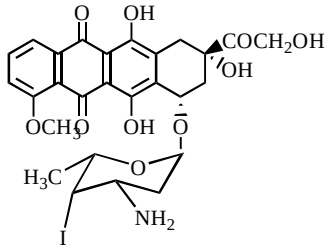

Iododoxorubicin

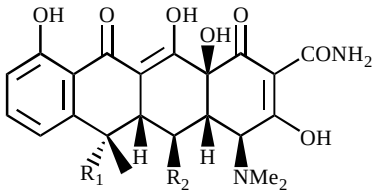

Tetracycline R_1=OH, R_2=H
Doxycycline R_1=H, R_2=OH

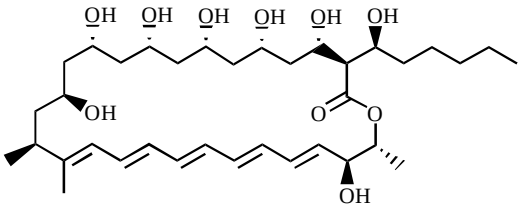

Filipin III (main component of filipin)

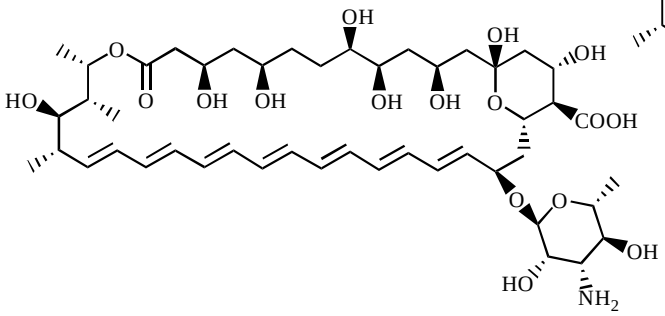

Amphotericin B

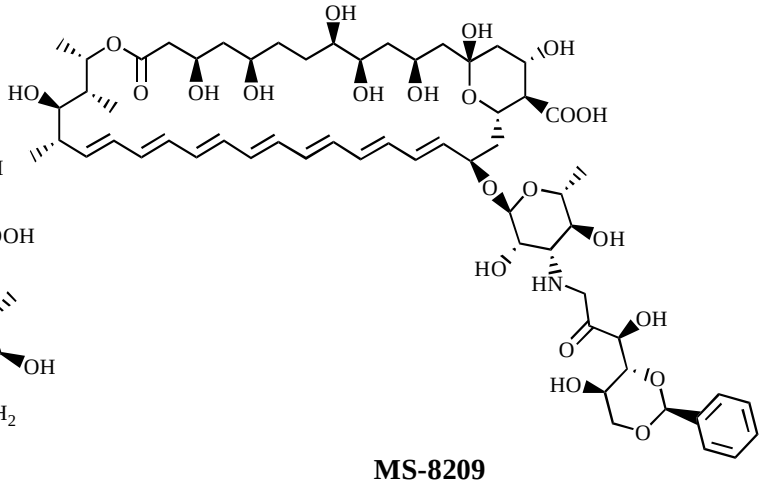

MS-8209

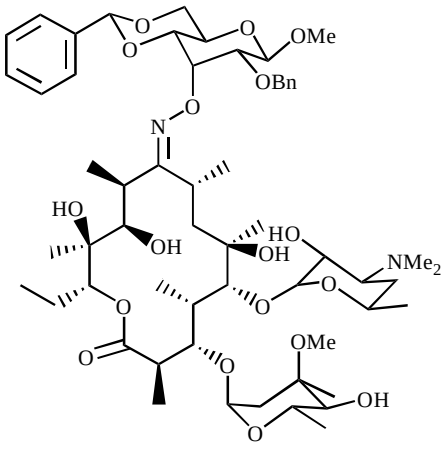

90

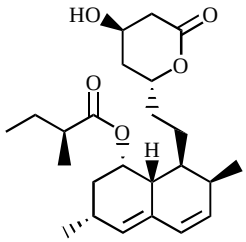

Lovastatin

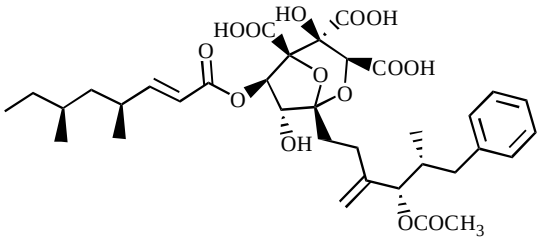

Squalestatin

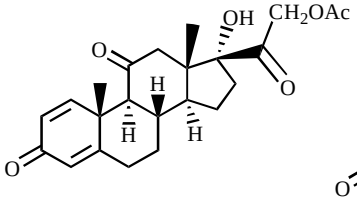

Prednisone acetate

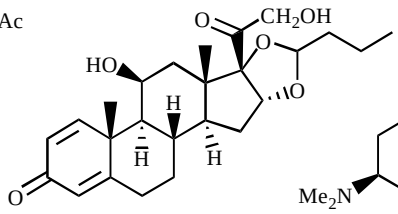

Budesonide

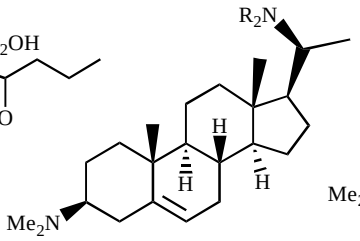

91a R=H
91b R=Me

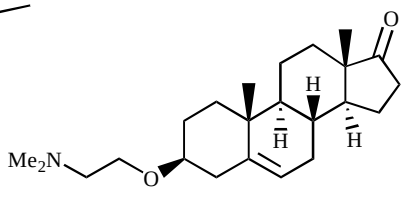

U18666A

Figure 14. Antibiotics, cholesterol-depleting agents and steroids

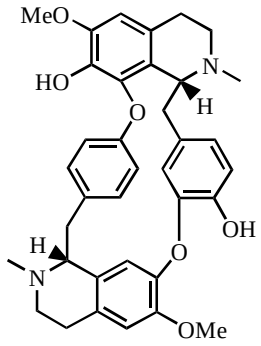

Bebeerine

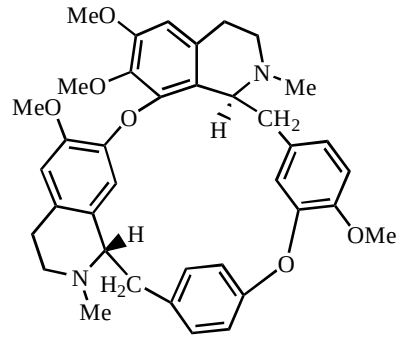

Tetrandrine

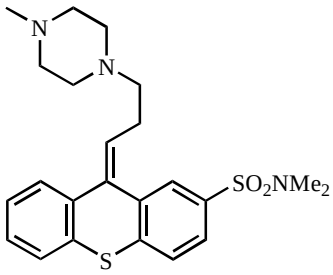

Thiothixene

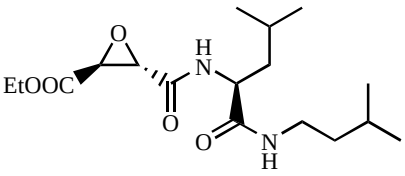

E64d

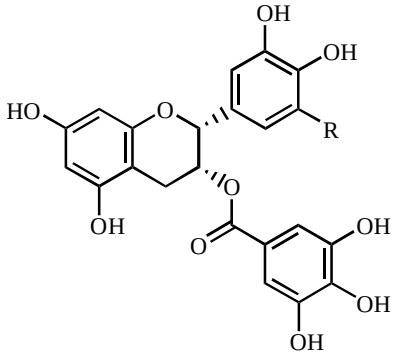

R=H Epicatechin 3-monogallate
R=OH Epigallocatechin 3-monogallate

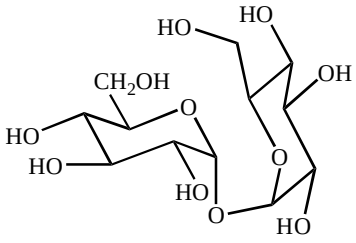

Trehalose

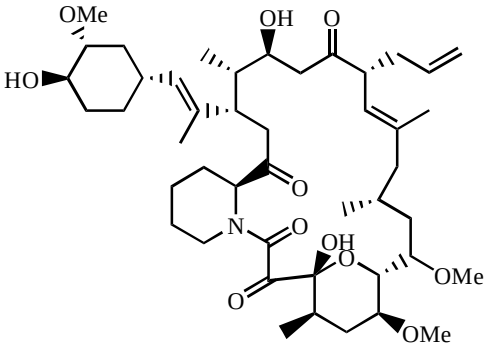

Tacrolimus

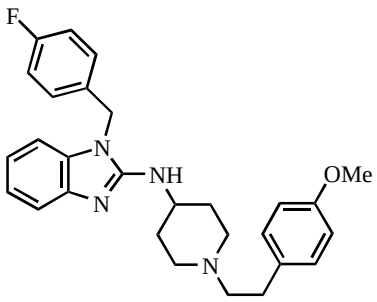

Astemizole

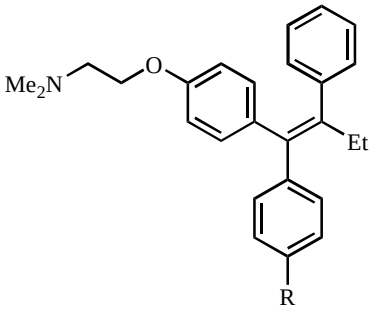

R=H Tamoxifen
R=OH 4-Hydroxytamoxifen

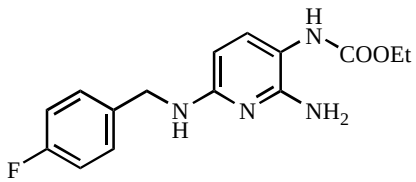

Flupirtine

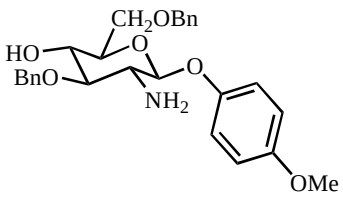

92

Figure 15. Miscellanea.